OPEN ACCESS Freely available online

PLoS BIOLOGY

Opposing Activities of LIT-1/NLK and DAF-6/Patched-Related Direct Sensory Compartment Morphogenesis in *C. elegans*

Grigorios Oikonomou[1], Elliot A. Perens[1], Yun Lu[1], Shigeki Watanabe[2], Erik M. Jorgensen[2], Shai Shaham[1]*

1 Laboratory of Developmental Genetics, The Rockefeller University, New York, New York, United States of America, **2** Howard Hughes Medical Institute, Department of Biology, University of Utah, Salt Lake City, Utah, United States of America

Abstract

Glial cells surround neuronal endings to create enclosed compartments required for neuronal function. This architecture is seen at excitatory synapses and at sensory neuron receptive endings. Despite the prevalence and importance of these compartments, how they form is not known. We used the main sensory organ of *C. elegans*, the amphid, to investigate this issue. *daf-6*/Patched-related is a glia-expressed gene previously implicated in amphid sensory compartment morphogenesis. By comparing time series of electron-microscopy (EM) reconstructions of wild-type and *daf-6* mutant embryos, we show that *daf-6* acts to restrict compartment size. From a genetic screen, we found that mutations in the gene *lit-1*/Nemo-like kinase (NLK) suppress *daf-6*. EM and genetic studies demonstrate that *lit-1* acts within glia, in counterbalance to *daf-6*, to promote sensory compartment expansion. Although LIT-1 has been shown to regulate Wnt signaling, our genetic studies demonstrate a novel, Wnt-independent role for LIT-1 in sensory compartment size control. The LIT-1 activator MOM-4/TAK1 is also important for compartment morphogenesis and both proteins line the glial sensory compartment. LIT-1 compartment localization is important for its function and requires neuronal signals. Furthermore, the conserved LIT-1 C-terminus is necessary and sufficient for this localization. Two-hybrid and co-immunoprecipitation studies demonstrate that the LIT-1 C-terminus binds both actin and the Wiskott-Aldrich syndrome protein (WASP), an actin regulator. We use fluorescence light microscopy and fluorescence EM methodology to show that actin is highly enriched around the amphid sensory compartment. Finally, our genetic studies demonstrate that WASP is important for compartment expansion and functions in the same pathway as LIT-1. The studies presented here uncover a novel, Wnt-independent role for the conserved Nemo-like kinase LIT-1 in controlling cell morphogenesis in conjunction with the actin cytoskeleton. Our results suggest that the opposing *daf-6* and *lit-1* glial pathways act together to control sensory compartment size.

Citation: Oikonomou G, Perens EA, Lu Y, Watanabe S, Jorgensen EM, et al. (2011) Opposing Activities of LIT-1/NLK and DAF-6/Patched-Related Direct Sensory Compartment Morphogenesis in *C. elegans*. PLoS Biol 9(8): e1001121. doi:10.1371/journal.pbio.1001121

Academic Editor: Gian Garriga, UC Berkeley, United States of America

Received January 14, 2011; **Accepted** June 28, 2011; **Published** August 9, 2011

Copyright: © 2011 Oikonomou et al. This is an open-access article distributed under the terms of the Creative Commons Attribution License, which permits unrestricted use, distribution, and reproduction in any medium, provided the original author and source are credited.

Funding: This work was supported by NIH grants 1R01HD052677, 1R01NS073121, and 5R01NS064273 to SS, and NIH (NS034307) and NSF (0920069) to EMJ. The funders had no role in study design, data collection and analysis, decision to publish, or preparation of the manuscript.

Competing Interests: The authors have declared that no competing interests exist.

Abbreviations: Dyf, dye-filling defective; EM, electron microscopy; EMS, ethyl methanesulfonate; fEM, Fluorescence Electron Microscopy; GFAP, glial fibrillary acidic protein; NLK, Nemo-like kinase; NLS-RFP, nuclearly localized dsRed fluorescent protein; PALM, photo-activated localization microscopy; SDS, sodium-dodecylsulfate; SNP, single nucleotide polymorphism; WASP, Wiskott-Aldrich syndrome protein; WIP, WASP interacting protein.

* E-mail: shaham@rockefeller.edu

Introduction

Sensory organs are the gates through which information flows into the nervous system. In many sensory organs, specialized glial cells form a chemically isolated compartment around neuronal receptive endings [1,2]. For example, in the skin, the mechano-sensory Pacinian corpuscles consist of an unmyelinated nerve ending that is surrounded by lamellae formed by a modified Schwann glial cell [3]. In the olfactory epithelium, sensory neurons are ensheathed by glia-like sustentacular cells [4,5]. In the inner ear, hair cells are surrounded by Deiter's cells, which express the glial marker glial fibrillary acidic protein (GFAP) [6]; and in the vertebrate eye, retinal pigmented epithelial cells contact photoreceptor cell cilia [7]. At least in some cases, the integrity of the glial compartment is essential for proper sensory neuron function [8]. Glial compartments also enclose excitatory neuronal synapses in the cerebellum and hippocampus [9,10], and are thought to be important for synaptic function through limiting neurotransmitter diffusion, and regulating levels of synaptic effectors. Despite the prevalence of such glial compartments, little is known about their development.

To determine how such compartments form, we turned to the major sense organ of the nematode *Caenorhabditis elegans*, the amphid. *C. elegans* has two bilaterally symmetric amphids located in the head [11]. Each amphid consists of 12 sensory neurons, which mediate many of the behavioral responses of the animal, and two glial cells, the sheath and socket glia (Figure 1A, top). Amphid neurons are bipolar, projecting an axon into the nerve ring (the main neuropil of the animal) and extending a dendrite anteriorly to the tip of the nose. The two amphid glia also extend anterior processes collateral to the dendrites. At the nose tip, sheath and socket glia form discrete single-cell tubular channels

Author Summary

The nervous system of most animals consists of two related cell types, neurons and glia. A striking property of glia is their ability to ensheath neuronal cells, which can help increase the efficiency of synaptic communication between neurons. Sensory neuron receptive endings in the periphery, as well as excitatory synapses in the central nervous system, often lie within specialized compartments formed by glial processes. Despite the prevalence of these compartments, and their importance for neuronal function and signal transmission, little is known about how they form. We have used the amphid, the main sensory organ of the worm *Caenorhabditis elegans*, to investigate glial sensory compartment morphogenesis. We demonstrate that the glia-expressed gene *daf-6*/Patched-related acts to restrict the size of the sensory compartment, while the Nemo-like kinase *lit-1* acts within glia in the opposite direction, to promote sensory compartment expansion. We show that LIT-1 localizes to the sensory compartment through a highly conserved domain. This domain can interact both with actin, which outlines the compartment, and with the regulator of actin polymerization WASP, which acts in the same pathway as *lit-1*. We postulate that Nemo-like kinases could have broader roles as regulators of cellular morphogenesis, in addition to their traditional role in regulating the Wnt signaling pathway.

joined by adherens junctions (Figure 1A bottom). The resulting two-cell channel compartment is open to the environment anteriorly and surrounds and isolates the ciliated endings of specific amphid sensory neurons. The socket portion of the channel is lined with cuticle and serves as a conduit for cilia to sample the animal's environment [11]. The sheath glial cell, however, is an active secretory cell [11], releasing extracellular matrix proteins, required for sensory neuron function, into the sheath glia channel [8].

Previous studies demonstrated that the morphogenesis of this compartment depends on the Patched-related gene *daf-6* [12–14], which acts within glia [14,15]. Although the primary defects in *daf-6* mutants were not characterized, these studies demonstrated that glial compartment formation employs mechanisms shared with the genesis of other tubular structures in the animal, including the vulva and excretory system [14]. Similarly, the *C. elegans* Dispatched-related protein CHE-14 seems to play important roles in the formation of the amphid sensory compartment and other tubular organs [14,16].

Here we demonstrate a primary function for *daf-6* in restricting sensory compartment size and show that the conserved MAP kinase LIT-1/NLK acts in counterbalance to DAF-6 to promote compartment expansion. Although LIT-1 is an important component of the Wnt signaling pathway in *C. elegans* [17], our studies argue against a role for Wnt in compartment size control. However, the previously characterized LIT-1 activator MOM-4/TAK1 is important for amphid sensory compartment morphogenesis. LIT-1 and MOM-4 co-localize to the amphid sensory compartment, and LIT-1 localization requires its highly conserved carboxy-terminal region. We demonstrate that this C-terminal domain physically interacts with actin and with the Wiskott-Aldrich syndrome protein (WASP), a regulator of actin polymerization [18]. Actin is highly enriched around the amphid pocket, and WASP appears to act in the same pathway as LIT-1 to influence compartment morphogenesis.

Our studies reveal two opposing activities, one mediated by DAF-6, the other by LIT-1, which, together with glial cytoskeletal proteins, drive sensory compartment morphogenesis.

Results

daf-6/Patched-Related Inhibits Amphid Sensory Channel Growth

The amphid sheath glial cell forms a compartment that surrounds the ciliated endings of amphid sensory neurons, constraining them into a tight bundle (Figure 1A–C). Within this bundle, 10 sensory cilia are stereotypically arranged in three successive columns containing 3, 4, and 3 cilia, respectively (Figure 1C; [11]). We previously reported the cloning and characterization of *daf-6*, a Patched-related gene required for amphid channel morphogenesis [14]. In *daf-6* mutant adults, the amphid channel is grossly enlarged, the socket and sheath glia channels are not continuous, and distal portions of sensory cilia are neither bundled nor exposed to the environment (Figure 1D and 1E).

At least two interpretations of this phenotype are possible: First, *daf-6* might act to open the sheath glia channel at its anterior end. Thus in *daf-6* mutants, the channel pocket would form but would remain sealed, and would continuously enlarge as matrix material is deposited. Second, *daf-6* might act to constrain the luminal diameter of the sheath glia channel. Thus, in *daf-6* mutants, the sheath and socket glia would properly align and form an open compartment, yet without lateral constraints on its size, the sheath channel would expand circumferentially. In this latter model, loss of the sheath-socket junction would be a later secondary defect.

To discriminate between these possibilities, we used electron microscopy (EM) to follow the development of amphid sensory compartments in wild-type and *daf-6*(*e1377*) mutant embryos. We used high-pressure freezing to fix embryos at several time points between 300 and 450 min post-fertilization, the time period during which the amphid is generated [19], collected serial sections, and assessed channel morphology.

By 380 min, sensory dendrites that have not yet formed cilia are evident in wild-type embryos. The tips of these dendrites are laterally ensheathed by the sheath glial cell, but the sheath cell also forms a cap blocking the anterior portion of the compartment and preventing access of neuronal processes to the socket (Figure S1).

By 400 min, a well-defined amphid primordium is formed in wild-type embryos (Figures 1F and S1). The sheath glia cap is gone and the open channel is continuous with the socket glia channel. At this stage, the socket channel is devoid of neuronal processes as dendritic tips have yet to extend cilia. Instead, a dense arrangement of filaments traverses the socket channel and forms a link between the tips of the sensory dendrites and the outside of the embryo (asterisk in Figure 1F). These filaments are consistent with an extracellular matrix proposed to anchor dendrites during retrograde extension [20]. Although cilia have not yet formed, structures resembling basal bodies (the initial sites of cilia construction) are visible at dendrite endings (arrow in Figure 1F).

In *daf-6* mutant embryos, the initial stages of amphid development are unperturbed ($n = 3$). By 400 min, the sheath and socket channels are aligned and open. Dendrites lacking cilia, but containing basal body-like structures, reside within the sheath channel, while filaments emanating from the dendrite tips and traversing the sheath and socket channels are seen (Figure 1H). However, only slightly later, at 420 min and before cilia have formed, bloating of the amphid sheath channel is apparent, and dendrites begin to unbundle (Figure 1I, compare to Figure 1G).

These studies indicate that *daf-6* is not required for aligning the sheath and socket channels or for opening the amphid sensory compartment. Rather, *daf-6* seems to function in restricting compartment diameter.

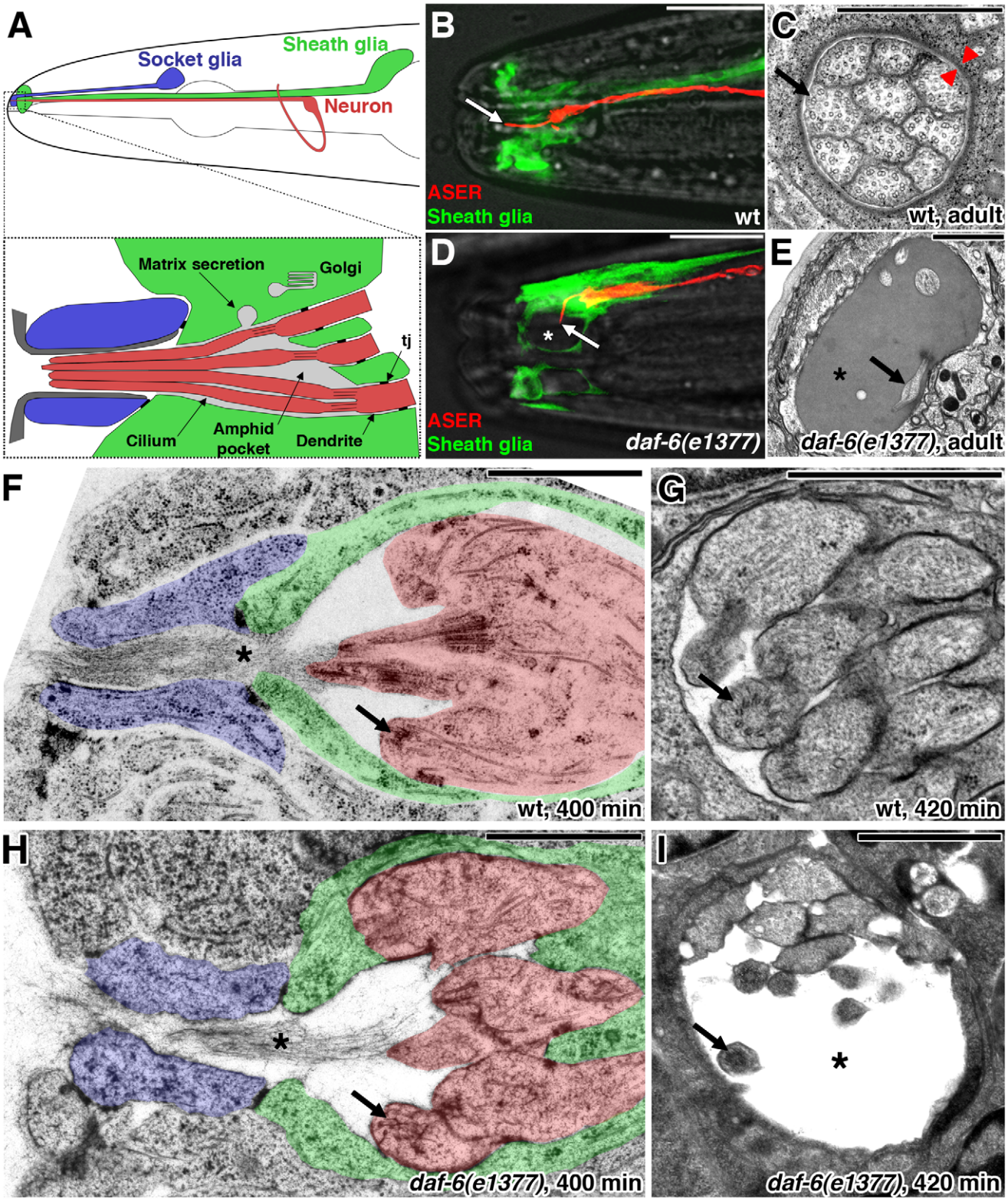

Figure 1. *daf-6* restricts amphid sensory compartment size. In longitudinal sections and diagrams (A, B, D, F, and H) anterior is left. White scale bars, 10 μm. Black scale bars, 1 μm. (A) Schematic of the *C. elegans* amphid. Top: Each amphid consists of 12 neurons (only one is depicted here) and two glial cells, the sheath and the socket. Bottom: Detail of the anterior tip of the amphid. Matrix is secreted by the Golgi apparatus. tj, tight junction. Adapted from [13]. (B, D) The ASER neuron and the amphid sheath glia visualized, respectively, with mCherry (red; driven by the *gcy-5* promoter) and GFP (green; driven by the *T02B11.3* amphid sheath promoter [32] in a wild-type (B) or *daf-6*(*e1377*) (D) animal (transgenes *nsEx2766* and *nsEx2752*, respectively)). The ASER neuron extends a single cilium through the length of the amphid channel in the wild type (arrow). In the mutant, the cilium is bent and not exposed to the environment, and the amphid pocket is bloated (asterisk). (C, E) Electron micrograph of a cross-section through the anterior portion of the amphid sheath glia channel in an adult wild-type animal (C) or a *daf-6*(*e1377*) adult mutant (E). Arrow in (C), sensory cilium. Red

arrowheads indicate subcortical electron dense material. Arrow in (E), bent cilium. Asterisk, bloated sheath glia channel. Note difference in magnification between (C) and (E). (F, H) Longitudinal section through the amphid primordium of a wild-type (F) or *daf-6*(*e1377*) (H) embryo at approximately 400 min of development. Asterisk, filaments. Arrow, basal body. (G, I) Cross-section through the amphid primordium of a wild-type (G) or *daf-6*(*e1377*) (I) embryo at approximately 420 min of development. Arrow, basal body. Asterisk, bloated channel. Note difference in magnification between (G) and (I). See also Figure S1.
doi:10.1371/journal.pbio.1001121.g001

Loss of *lit-1*/NLK Restores Amphid Sensory Compartment Morphology and Function to *daf-6* Mutants

The abnormal expansion of the amphid sensory compartment in *daf-6* mutants suggests that active processes promote compartment expansion and that these processes are balanced by *daf-6* activity during development. We surmised that mutations in genes promoting compartment expansion might, therefore, counteract the loss of *daf-6* and restore compartment size and function.

To identify such genes, we screened for mutants able to generate a normal compartment in the absence of *daf-6* function, taking advantage of an easily scored *daf-6* mutant defect: the inability to form dauer larvae. Dauer is an alternative developmental state induced by starvation and perception of high concentration of dauer pheromone. Dauer animals are highly resistant to environmental insults and can survive in the presence of 1% sodium-dodecylsulfate (SDS) [21]. *daf-6* mutants fail to become dauer larvae, presumably due to their sensory deficits [22], and are thus killed by exposure to SDS. We therefore randomly mutagenized animals homozygous for the strong loss-of-function *daf-6*(*e1377*) allele [14] using ethyl methanesulfonate (EMS), allowed F2 animals to starve, and treated them with SDS. Resistant animals could have suppressed the *daf*-6 amphid sensory compartment defects or could have constitutively activated a more downstream step in dauer formation. To distinguish between these mutant classes, we examined the ability of amphid sensory neurons to fill with dye provided in the medium. When exposed to a solution of the lipophilic dye DiI, wild-type animals readily take up the dye into exposed amphid neurons. *daf-6* animals fail to do so, presumably due to their defective amphid sensory compartments (Figure S2A–C) [13,23].

From a screen of 60,000 mutagenized genomes we identified seven mutants that survived SDS treatment and that dye filled properly. We further characterized one of these *daf-6* suppressors, given the allele designation *ns132*. As shown in Figure 2A, approximately 40% of *ns132; daf-6*(*e1377*) animals are able to take up dye in at least one amphid. Likewise, the *ns132* allele was able to suppress amphid channel defects in another *daf-6* mutant, *n1543*, supporting the notion that *ns132* is a bypass suppressor (Figure 2A).

To further confirm the rescue of the *daf-6* amphid defects in *ns132*; *daf-6*(*e1377*) animals, we examined amphid sensory compartments using fluorescence microscopy. We found that cilia in these double mutants projected through a compartment of normal appearance (Figure 2B, compare to Figure 1D). In addition, *ns132*; *daf-6*(*e1377*) individuals that displayed normal dye filling in one of the two amphids had one amphid channel that resembled a wild-type channel by EM serial reconstruction (Figure 2C; $n = 3$). Interestingly, even in rescued amphids, cilia packing was more variable compared to the regular 3:4:3 packing observed in wild-type animals, and the amphid sensory compartment was somewhat wider than normal (Figure 2C, compare to Figure 1C), perhaps reflecting a partial suppression of the *daf-6* defects.

We used single nucleotide polymorphism (SNP) mapping and transgenic rescue methods (Figure S2D) to identify the gene defective in *ns132* animals as *lit-1*. *lit-1* encodes a Ser/Thr MAP kinase that is highly conserved from *C. elegans* to mammals. Supporting this assignment, a genomic region containing *lit-1* restored dye-filling defects to *ns132*; *daf-6*(*e1377*) animals (Figures 2A and S2E), as did a transgene in which the *lit-1* promoter region (2.5 kb upstream of the *lit-1* start codon) drives the *lit-1* cDNA (Figure 2A). Furthermore, a temperature-sensitive mutation in *lit-1*, *t1512*, also suppressed the dye-filling defects of *daf-6*(*n1543*) mutants (Figure 2A). Finally, we found that animals containing the *ns132* allele have a C-to-T mutation in the coding region of *lit-1*, converting codon 437, encoding glutamine, to a stop codon. This mutation is predicted to result in a truncated LIT-1 protein (Figure 2D) lacking the last 26 amino acids of the highly conserved carboxy-terminal (C-terminal) domain.

LIT-1 Functions in Amphid Glia During Compartment Formation

To determine in which cells *lit-1* functions to regulate compartment development, we first examined its expression pattern by generating animals harboring a transgene in which the *lit-1* promoter drives expression of a nuclearly localized dsRed fluorescent protein (NLS-RFP). We found that *lit-1* is expressed in amphid sheath glia (Figure 3A), among other cells. In addition, the expression pattern of this reporter partially overlaps with that of *ptr-10* (Figure 3B), a gene expressed in ensheathing glia of other sensory organs [24], suggesting that *lit-1* could act in compartment formation in other *C. elegans* sensory structures as well.

Next, we pursued cell-specific rescue experiments to determine in which cells *lit-1* can act to regulate compartment morphogenesis. We generated *lit-1*(*ns132*); *daf-6*(*e1377*) animals containing a transgene in which a *lin-26* promoter fragment drives expression of the *lit-1* cDNA in glia, but not neurons, of embryos at the time of amphid sensory compartment formation [25]. We found that transgenic animals were rescued (Figure 3C), supporting the notion that *lit-1* can act in glia to regulate compartment morphology. Importantly, expression of the *lit-1* cDNA in amphid sensory neurons during the time of amphid morphogenesis (using the *dyf-7* promoter; [20]) failed to rescue *lit-1*(*ns132*); *daf-6*(*e1377*) animals (Figure 3C).

To determine whether *lit-1* can control amphid sensory compartment structure after compartment formation is complete, we examined *lit-1*(*ns132*); *daf-6*(*e1377*) animals expressing the *lit-1* cDNA under the control of the sheath glia-specific *vap-1* promoter. *vap-1* expression begins in late embryos [14], after the compartment has formed. We found that these transgenic animals were not rescued (Figure 3C), supporting the conclusion that *lit-1* is required within amphid sheath glia at the time of amphid morphogenesis to influence compartment formation.

Finally, to ascertain whether the kinase activity of LIT-1 is required, we generated a mutant *lit-1* cDNA that disrupts the ATP binding domain (VALKK to VALGK) and which has been shown to eliminate LIT-1 kinase activity in vitro [17]. *lit-1*(*ns132*); *daf-6*(*e1377*) animals carrying a *lin-26* promoter::LIT-1(K97G) cDNA transgene still displayed 30% dye filling, similar to controls, suggesting that LIT-1 kinase activity is indeed required for glial compartment morphogenesis (Figure 3C). None of the transgenes used in Figure 3C had an effect on the dye filling of wild-type animals ($n > 100$).

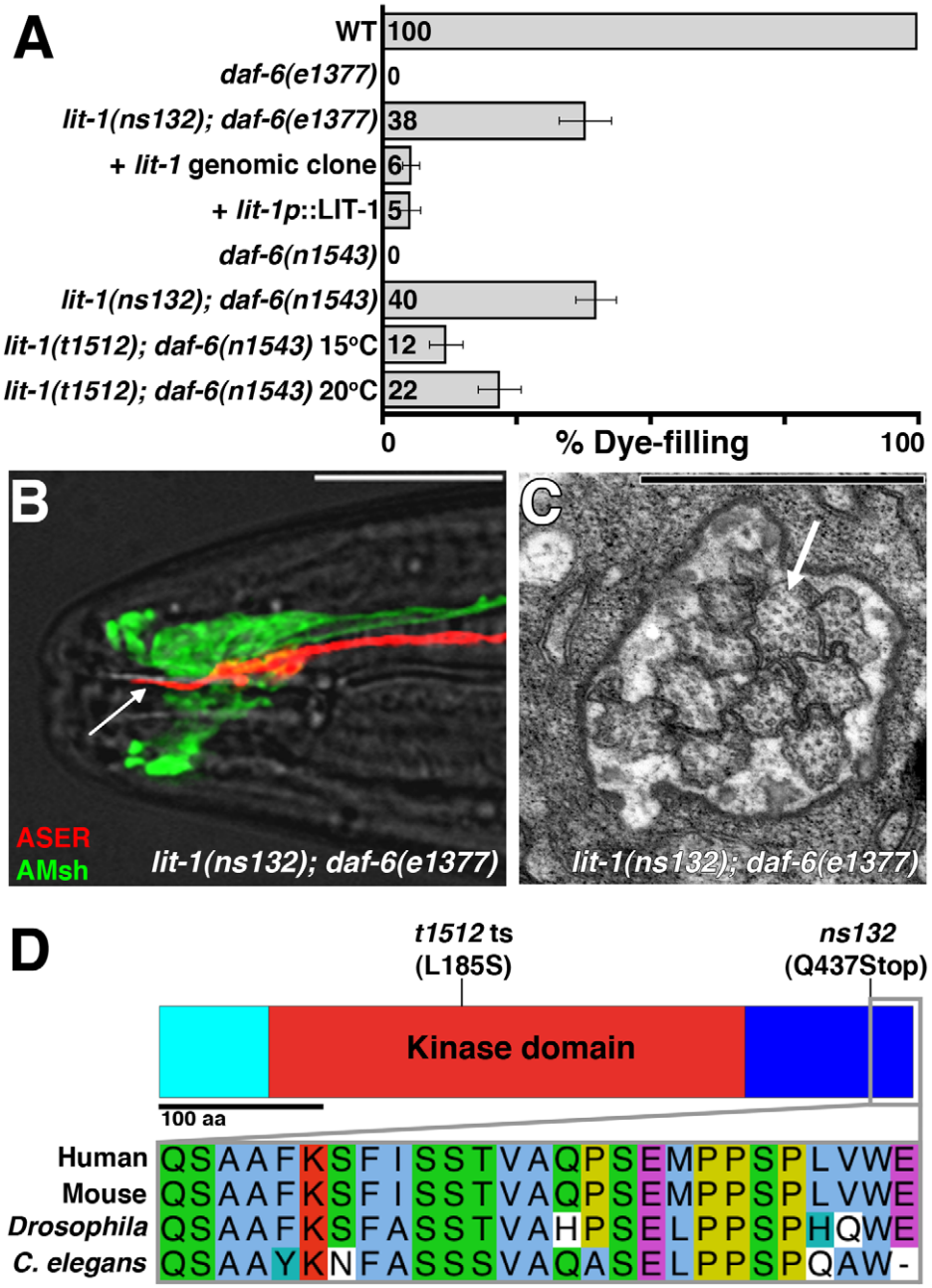

Figure 2. Loss of *lit-1* suppresses the loss of *daf-6*. (A) Dye-filling assay for indicated genotypes ($n \geq 90$). The *lit-1*(*t1512*) strain also contained the *unc-32*(*e189*) mutation. *unc-32*(*e189*) does not affect dye filling (unpublished data). Error bars, standard error of the mean (SEM). (B) The ASER neuron and the amphid sheath glia, visualized with mCherry (red) and GFP (green), respectively, in a *lit-1*(*ns132*); *daf-6*(*e1377*) animal (transgene *nsEx2761*). Arrow, ASER cilium. Left is anterior. Scale bar, 10 µm. (C) Electron micrograph of a cross-section through the amphid sheath channel of a *lit-1*(*ns132*); *daf-6*(*e1377*) adult animal. Arrow, cilium. Scale bar, 1 µm. (D) Top: Schematic of the LIT-1 protein. Light blue, non-conserved N-terminal domain. Red, conserved kinase domain. Dark blue, conserved C-terminal domain. Bottom: Alignment of the region truncated in *lit-1*(*ns132*) from different species. See also Figure S2.
doi:10.1371/journal.pbio.1001121.g002

lit-1 Promotes Amphid Sensory Compartment Expansion

Since *daf-6* normally acts to restrict amphid sensory compartment expansion, the observation that *lit-1* mutations suppress *daf-6* suggests that *lit-1* may normally promote compartment growth. Consistent with this idea, the *lit-1*(*ns132*) allele enhances the dye-filling defects of *che-14*(*ok193*) mutants (Figure 4A). CHE-14 protein is similar to the *Drosophila* and mammalian protein Dispatched, and is important for apical secretion and amphid sensory compartment morphogenesis [16], suggesting a role in lumen expansion. The enhancement of *che-14* defects by *lit-1*(*ns132*) suggests that both genes may be involved in this process.

To further test the idea that *lit-1* promotes compartment expansion, we examined *lit-1*(*ns132*) single mutants for dye-filling abnormalities; however, no defects were observed (Figure 4B), suggesting that amphid morphology in these animals may be normal. However, two observations suggest that *ns132* is a weak

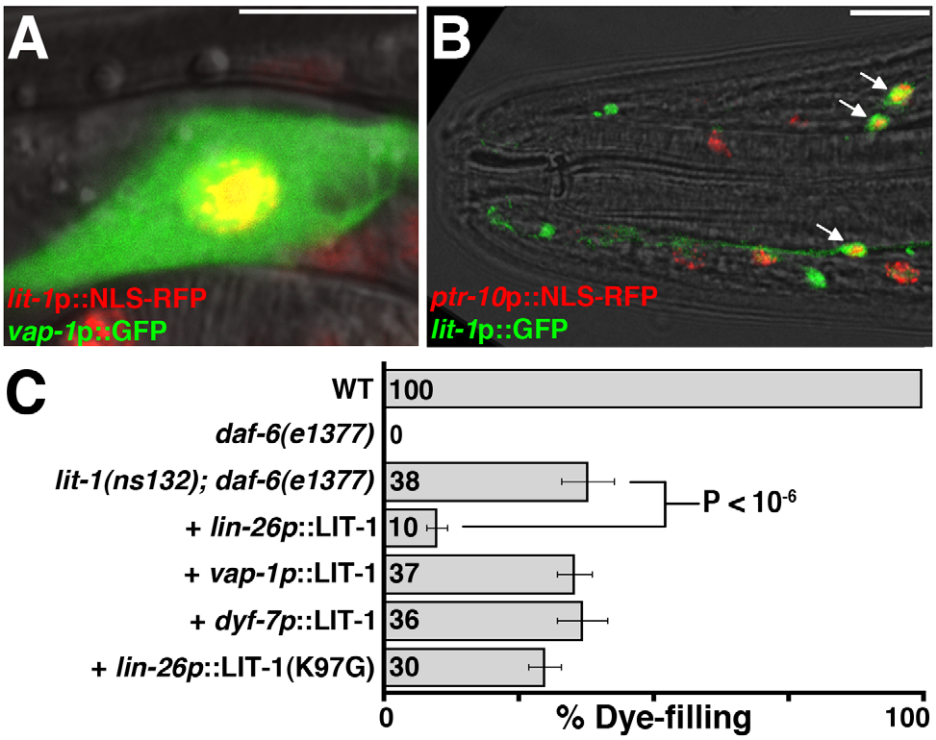

Figure 3. Suppression of *daf-6* mutations requires loss of *lit-1* in glia. (A) Image of an amphid sheath glial cell body expressing *lit-1*p::NLS-RFP (red; in nucleus) and *vap-1*p::GFP (green) (transgene *nsEx2308*). Yellow, overlapping expression. Left is anterior. Scale bar, 10 μm. (B) Image of an adult (head) expressing *lit-1*p::GFP (green) and *ptr-10*p::NLS-RFP (red) (transgene *nsEx2159*). Arrows, cells with overlapping expression. Left is anterior. Scale bar, 10 μm. (C) Dye-filling assay for indicated genotypes ($n \geq 90$). None of the transgenes had an effect on the dye filling of wild type animals ($n > 100$, unpublished data). Error bars, SEM. *p* value calculated using Chi-squared test.
doi:10.1371/journal.pbio.1001121.g003

allele of *lit-1*. First, the *ns132* lesion truncates only 26 amino acids from the C-terminus of the LIT-1 protein and leaves the kinase domain intact (Figure 2D). Second, null alleles of *lit-1* are embryonic lethal [17,26], whereas *ns132* mutants are fully viable.

To examine the consequences of more severe defects in *lit-1* function, we turned to animals homozygous for the *lit-1(t1512)* temperature-sensitive allele. *lit-1*(*t1512*ts) animals grow nearly normally at 15°C, but exhibit early embryonic lethality at 25°C [26]. At 20°C, some *lit-1*(*t1512*ts) embryos escape lethality and grow to adulthood. We reasoned that in some of these escapers, LIT-1 activity could be low enough to allow us to discern defects in amphid morphogenesis. Indeed, as shown in Figure 4B, nearly 50% of *lit-1*(*t1512*ts) adults grown at 20°C exhibit defects in a sensitized amphid dye-filling assay (this assay was developed to detect weak defects in dye filling; see Experimental Procedures). These results suggest that amphid structure, and perhaps compartment morphogenesis, has been perturbed in these mutants.

To assess whether compartment morphology is indeed perturbed, we performed serial-section EM on dye-filling defective adult *lit-1*(*t1512*ts) animals raised at 20°C ($n = 3$). Whereas in wild-type animals a cross-section through the sheath channel immediately posterior to the socket-sheath boundary (yellow line in Figure 4C) reveals the stereotypical 3:4:3 arrangement of the 10 channel cilia, in *lit-1*(*t1512*ts) mutants (Figure 4D), the amphid sensory compartment has a smaller diameter and contains fewer cilia. Fewer cilia are also found in the socket channel in *lit-1*(*t1512*ts) animals (unpublished data). Furthermore, in wild-type animals, cross-sections roughly 1 μm posterior to the sheath-socket junction (blue line in Figure 4C) reveal a less packed arrangement of cilia that are loosely surrounded by the sheath glia membrane; by contrast, in *lit-1*(*t1512*ts) animals the sheath glia is tightly wrapped around individual cilia (arrowheads in Figure 4D), consistent with the idea that compartment diameter is reduced. Importantly, despite the posterior displacement of some cilia in *lit-1*(*t1512*ts) animals, the total number of cilia is normal (blue section in Figure 4D).

Taken together, the *che-14*, dye-filling, and EM studies suggest that *lit-1* opposes *daf-6* by promoting channel expansion during amphid morphogenesis.

Mutation of the MAP Kinase Kinase Kinase *mom-4*/TAK1 Also Suppresses the Compartment Defects of *daf-6* Mutants

The kinase activity of LIT-1 was previously shown to depend on MOM-4/TAK1, a MAP kinase kinase kinase. MOM-4 increases LIT-1 kinase activity in vitro and mutations in *mom-4* interact genetically with mutations in *lit-1* during anterior/posterior polarity establishment in early embryos [27]. We therefore tested whether mutations in *mom-4* could also suppress the dye-filling defects of *daf-6* mutants. While complete loss of *mom-4*, like loss of *lit-1*, leads to early embryonic lethality, some animals homozygous for a temperature-sensitive allele of *mom-4*, *ne1539*ts, can escape lethality. We found that whereas only 1% of *mom-4*(*ne1539*ts); *daf-6*(*e1377*) double-mutant escapers grown at 15°C exhibit suppression of the *daf-6* dye-filling defect, 18% of surviving animals grown at 20°C can take up dye ($p < 10^{-6}$, Chi-squared test; Figure 5A). This observation suggests that *mom-4* acts similarly to *lit-1* in compartment expansion.

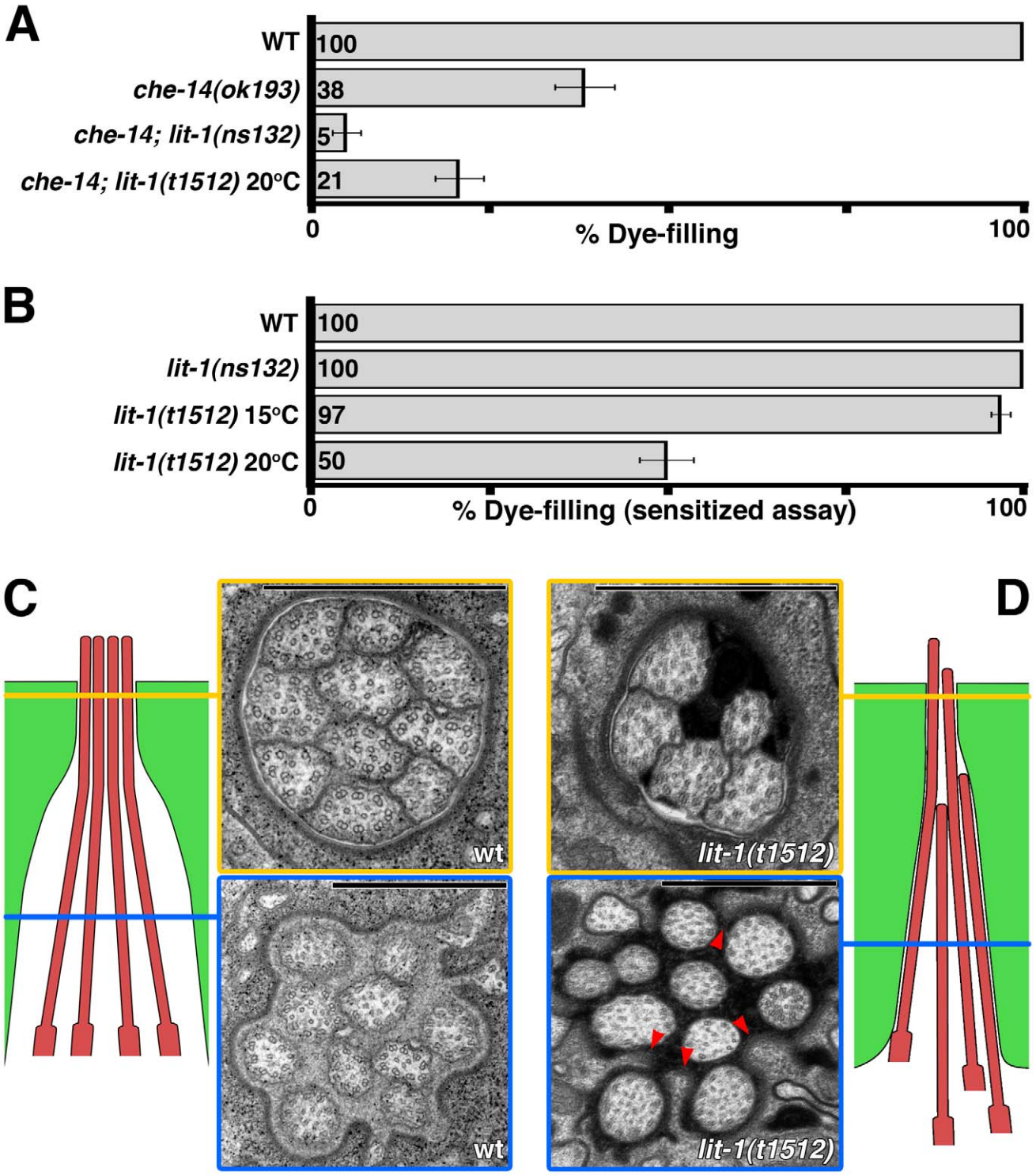

Figure 4. LIT-1 is required for amphid sensory compartment morphogenesis. (A, B) Dye filling in animals carrying the indicated mutations ($n \geq 100$). Error bars, SEM. In (B) a sensitized dye-filling assay was used (see Experimental Procedures). (C) Left: Schematic of the arrangement of the cilia (red) and the sheath glial channel (green) in a wild-type adult animal. Not all cilia are depicted. Right: electron micrograph of cross-sections of the amphid channel. Section outlined in yellow is just below the socket-sheath junction; blue outlined section is approximately one micron posterior. Scale bars, 1 μm. (D) Same as in (C), but for a dye-filling defective *lit-1*(*t1512*) adult animal. The panel arrangement is a reflection of the one in (C). Arrowheads, tight ensheathment of individual cilia by the sheath glia. Scale bars, 1 μm.
doi:10.1371/journal.pbio.1001121.g004

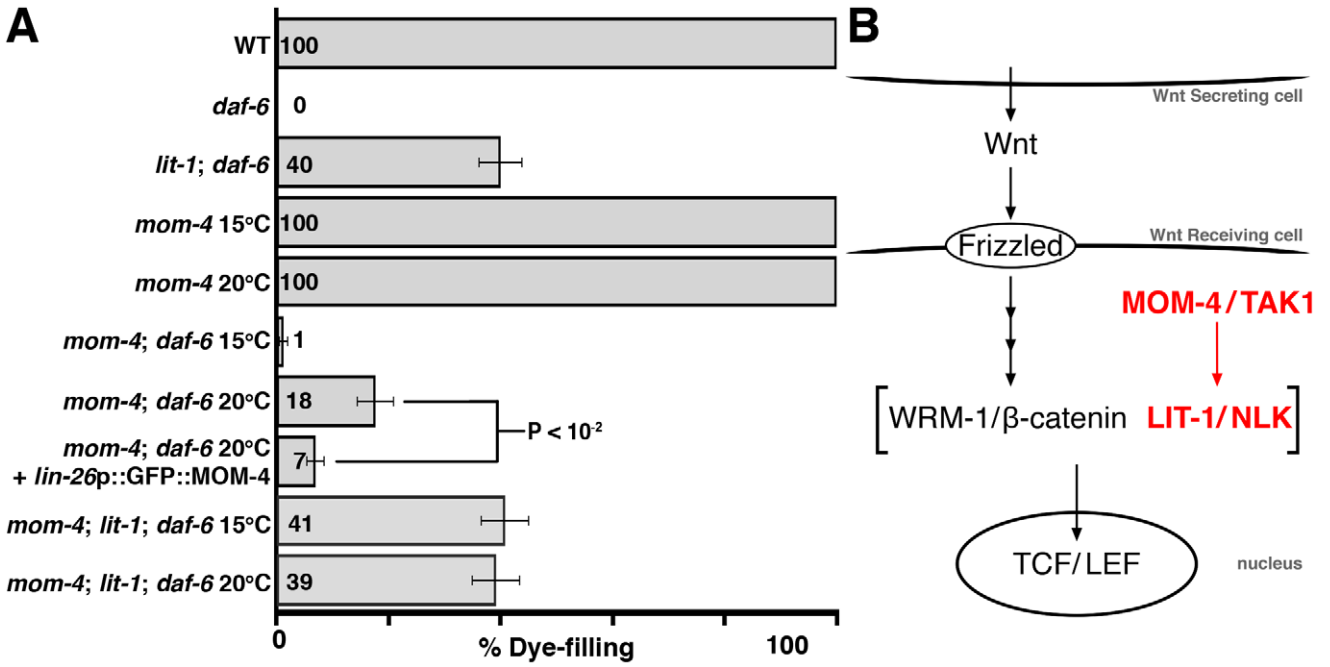

Figure 5. *mom-4*/TAK1 mutations suppress the loss of *daf-6*. (A) Dye filling in animals of the indicated genotypes ($n \geq 90$). The alleles used are: *daf-6*(*n1543*), *lit-1*(*ns132*), *mom-4*(*ne1539*). *daf-6* is marked with *unc-3*(*e151*) in all strains except for *mom-4; daf-6*. *unc-3*(*e151*) does not affect dye filling (unpublished data). Error bars, SEM. *p* value calculated using Chi-squared test. (B) Schematic of Wnt signaling during endoderm specification in *C. elegans*. In contrast to the LIT-1 MAPK module (red), Wnt signaling does not appear to be involved in amphid sheath channel formation (see text and Table S1).
doi:10.1371/journal.pbio.1001121.g005

To test whether *mom-4*, like *lit-1*, acts within glia to regulate amphid morphogenesis, we constructed *mom-4*(*ne1539*ts); *daf-6*(*e1377*) double mutants expressing a *lin-26* promoter::GFP::*mom-4* cDNA transgene. When these animals were grown at 20°C, only 7% filled with dye (Figure 5A), consistent with the hypothesis that *mom-4* acts within glia during early amphid morphogenesis, similar to *lit-1*.

To assess whether *mom-4* and *lit-1* function in the same pathway to promote channel expansion, we examined dye filling in *daf-6* mutants that were also homozygous for both *lit-1*(*ns132*) and *mom-4*(*ne1539*ts) alleles. We found that the *mom-4*; *lit-1*; *daf-6* triple mutant is viable at both 15°C and 20°C and is not suppressed to a greater extent than *lit-1*; *daf-6* double mutants at either temperature (Figure 5A). This result is consistent with the idea that *lit-1* and *mom-4* function in the same pathway to control channel expansion, similar to their established roles in embryonic cell polarity.

The roles of *lit-1* and *mom-4* in Wnt signaling in *C. elegans* have been extensively studied [28,29]. In this context, MOM-4 activates LIT-1, which then forms a complex with the β-catenin WRM-1. The LIT-1/WRM-1 complex phosphorylates the *C. elegans* TCF/LEF transcription factor POP-1, resulting in reduction (but not elimination) of POP-1 nuclear levels and activation of transcription (Figure 5B) [17,27,30,31]. We therefore examined animals containing mutations in Wnt signaling components for defects in dye filling, or for suppression of the *daf-6* dye-filling defects. Surprisingly, mutations in Wnt-encoding genes, the *C. elegans* Wntless homolog *mig-14*, required for Wnt protein secretion, Wnt receptors, β-catenins, or *pop-1*/TCF/LEF, the main LIT-1 target in the Wnt signaling pathway, have no effect on dye filling and show no, or minimal, suppression of *daf-6* (Table S1).

Although we cannot eliminate the possibility that multiple redundant Wnt pathways contribute to channel formation and that these operate through LIT-1 targets other than POP-1, the most parsimonious interpretation of our data is that the MOM-4/LIT-1 kinase module operates independently of Wnt signaling to promote expansion of the amphid glial compartment.

LIT-1 and MOM-4 Proteins Localize to the Amphid Sensory Compartment

To determine where within the amphid sheath glia LIT-1 and MOM-4 are localized, we generated animals expressing either a rescuing GFP::MOM-4 or a rescuing GFP::LIT-1 fusion protein within amphid sheath glia using the *T02B11.3* amphid sheath promoter [32]. Strikingly, we found that both fusion proteins were tightly associated with the amphid sensory compartment (Figure 6A and 6B).

To determine whether LIT-1 localization requires functional *mom-4*, we examined localization of the GFP::LIT-1 fusion protein in *mom-4*(*ne1539*ts) single mutants at 20°C. GFP::LIT-1 was properly localized in all animals we observed ($n = 44$), suggesting that LIT-1 localizes to the sheath channel independently of its regulator.

The DAF-6 protein is mislocalized in animals lacking neuronal cilia, accumulating only at the sheath-socket junction rather than along the length of the sheath glia channel [14]. To examine whether LIT-1 also requires cilia to properly localize, we examined animals harboring a loss-of-function mutation in *daf-19*, which encodes a transcription factor required for ciliogenesis. Our previous EM studies demonstrated that, despite minor defects, a channel of normal length is generated in these mutants [14]. As shown in Figure 6C, in *daf-19* mutants, LIT-1 no longer lines the entire channel, but is restricted to its anterior aspect. Thus, neuronal signals are required for LIT-1 glial localization.

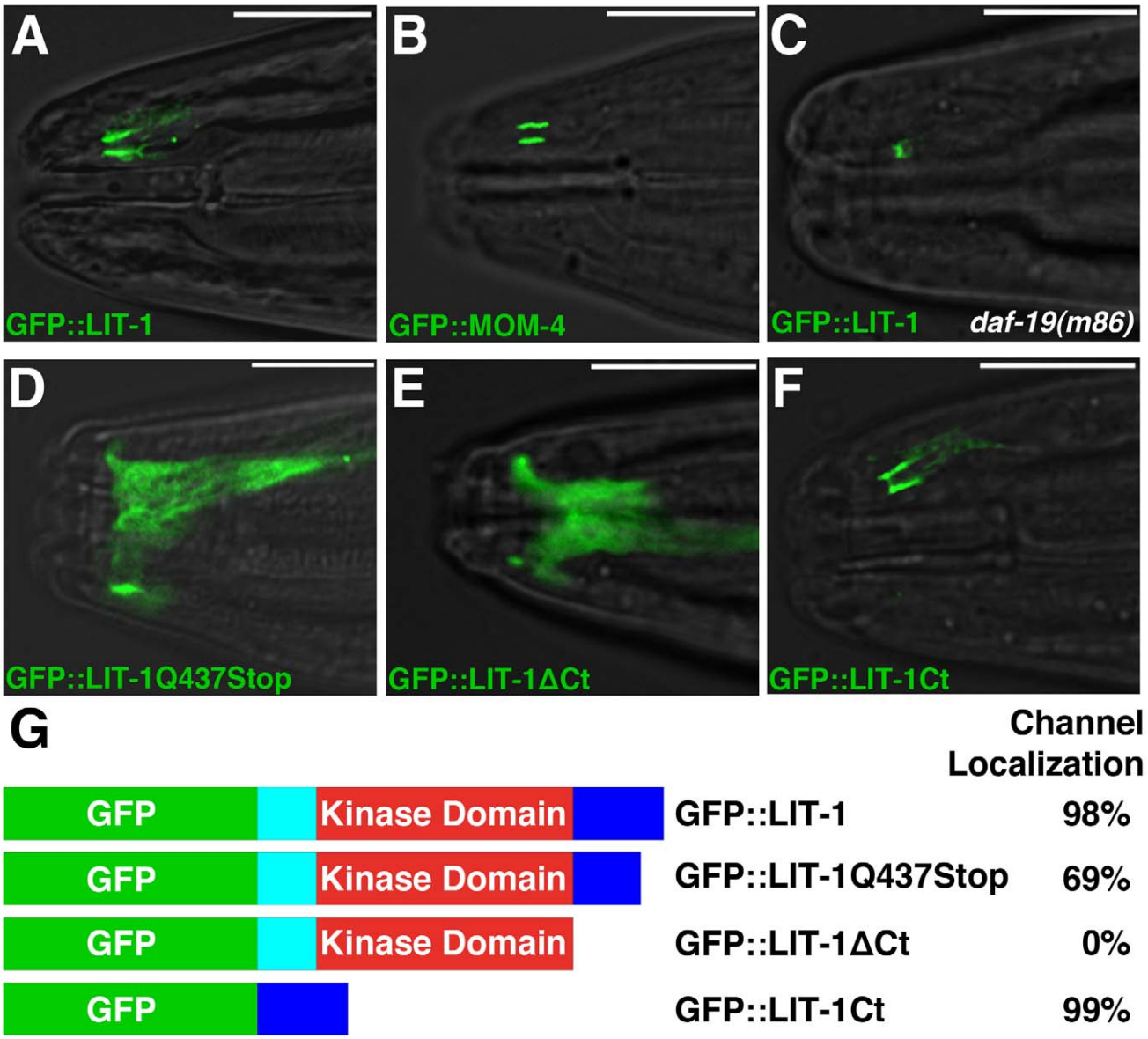

Figure 6. LIT-1 and MOM-4 localize to the amphid sensory compartment. (A–F) Images of adult animals expressing the indicated GFP fusion proteins. Animals are otherwise wild-type except in (C). *daf-19*(*m86*) animals also carried the *daf-16*(*mu86*) allele to prevent dauer entry. The *T02B11.3* amphid sheath promoter [32] was used to drive all constructs. Transgenes depicted: *nsEx2606* (A), *nsEx2840* (B), *nsEx2829* (C), *nsEx2609* (D), *nsEx2747* (E), and *nsEx2626* (F). Anterior is to the left. Scale bars, 10 μm. (G) Quantification of channel localization of indicated LIT-1 protein fusions ($n \geq 100$). See also Figure S3.
doi:10.1371/journal.pbio.1001121.g006

The C-Terminus of LIT-1 Is Necessary and Sufficient for Amphid Sensory Compartment Localization

The channel localization of LIT-1 raised the possibility that in *lit-1*(*ns132*) mutants, LIT-1 localization might be disrupted. To test this, we expressed GFP-tagged LIT-1(Q437Stop) (the mutation corresponding to *ns132*) in wild-type animals and examined its localization. While GFP::LIT-1 reproducibly lines the amphid sensory compartment, GFP::LIT-1(Q437Stop) fails to localize in about one-third of animals and is instead diffusely distributed throughout the cell (Figure 6D and 6G). This result suggests that the highly conserved C-terminal region of LIT-1 may be required for compartment localization. In addition, the fraction of animals in which GFP::LIT-1(Q437Stop) is mislocalized (31%, Figure 6G) mirrors the fraction of *daf-6* mutants suppressed by the *lit-1*(*ns132*) allele (Figure 2A), raising the possibility that mislocalization may account for the suppression we observed.

The observation that GFP::LIT-1(Q437Stop) still localizes to the amphid channel in some animals raised the possibility that the C-terminal 26 amino acids may represent only a portion of the full targeting domain. To test this idea, we generated animals expressing a GFP::LIT-1ΔCt fusion protein in which all sequences downstream of the kinase domain are deleted. We found that in these animals LIT-1 never accumulated at the amphid sensory compartment, and was diffusely distributed throughout the cell (Figure 6E and 6G), demonstrating that the C-terminal domain is necessary for LIT-1 compartment localization.

To determine whether the C-terminal domain of LIT-1 is sufficient for channel localization, we generated animals express-

ing a GFP::LIT-1 C-terminal domain fusion protein. Remarkably, we found that this fusion protein accumulated at the amphid sensory compartment in a pattern identical to that of full-length LIT-1 (Figure 6F and 6G).

Previous work showed that LIT-1 also localizes to the cell nucleus [30,33,34], and we found this to be the case for amphid sheath glia as well (Figure S3). However, disruption of the C-terminal domain of LIT-1 does not result in its exclusion from the nucleus (Figure S3), suggesting that nuclear functions of LIT-1 may not be abrogated in *lit-1*(*ns132*) mutants.

Although the C-terminal domain of LIT-1 is highly conserved from *C. elegans* to mammals, its function is not well studied. Our studies demonstrate that this domain is both necessary and sufficient for LIT-1 localization to the amphid sensory compartment, and suggest that proper localization is important for LIT-1 function in compartment formation.

ACT-4 Interacts with the C-terminal Domain of LIT-1 and Is Enriched around the Amphid Sensory Compartment

Because of the importance of the LIT-1 C-terminal domain in compartment localization, we used this domain as bait in a yeast two-hybrid screen with the aim of identifying proteins that interact with LIT-1.

From a screen of approximately 10^6 clones, we identified 26 positive clones (Table S2, Figure 7A). While some clones were isolated multiple times, others were found only once, suggesting that our screen was not saturated. We were intrigued that 4 of the 26 interacting clones identified encoded the *C. elegans* actin protein ACT-4. EM studies of the amphid sheath glia channel had previously shown that the channel is lined by an electron dense subcortical layer (red arrowheads in Figure 1C) [13]. A similar layer can be seen in other highly secreting cells such as pancreatic acinar cells and adrenal chromaffin cells. In these cells, this electron dense layer has been demonstrated to be enriched in actin [35,36].

To determine whether ACT-4 might be part of the electron-dense subcortical layer near the amphid sensory compartment, we examined animals expressing a GFP::ACT-4 fusion protein in amphid sheath glia. Strikingly, we found that although GFP::ACT-4 was seen throughout the cell, it was highly enriched at the amphid sensory compartment (Figure 7B). We wondered whether other actin proteins also accumulate at the channel and, therefore, generated animals expressing a protein fusion of GFP to ACT-1. Again, we found increased channel localization (unpublished data), suggesting that actin filaments may be components of the subcortical density.

To examine the localization pattern of ACT-4 at higher resolution, we used scanning EM coupled with photo-activated localization microscopy (PALM). In this method, serial sections are imaged by scanning EM and using single-molecule fluorescence of mEos::ACT-4 [37]. Images are then superimposed, using fiduciary markers (fluorescent gold beads), to reveal the subcellular localization of fluorescent proteins. As shown in Figure 7C, at the anterior portion of the amphid channel, where an electron dense subcortical region has been described, mEos::ACT-4 is localized near the sensory compartment membrane (blue trace). mEos::ACT-4 does not localize to the sensory compartment in more posterior sections (Figure 7D, 2 μm posterior to 7C), which should lack the subcortical electron density. These observations support the notion that actin is intimately associated with the glial sensory compartment and that the subcortical density may be composed at least in part of actin.

We also found that GFP::ACT-4 was properly localized in *lit-1*(*ns132*) mutants ($n = 50$), suggesting that actin accumulates around the sensory compartment independently of *lit-1*, and consistent with the possibility that actin may recruit LIT-1. To test this possibility we tried to disturb GFP::ACT-4 localization by treating the animals with an inhibitor of actin polymerization, cytochalasin D. After a 2 h incubation with 1 mM of the drug, the cell bodies of the sheath glia assumed a rounded morphology, indicative of breakdown of the actin cytoskeleton. However, the sensory compartment localization of neither GFP::ACT-4 nor GFP::LIT-1 was disturbed (unpublished data). This result suggests that the subcortical actin around the amphid channel could be part of a stable structure with a lower turnover rate than the rest of the actin cytoskeleton.

Similarly, LIT-1, MOM-4, and ACT-4 all localized to the sensory compartment in *daf-6*(*n1543*) mutants (Figure S4), suggesting that DAF-6 is not involved in recruiting these proteins.

The Actin Regulator WASP Binds LIT-1 and Is Required for Sensory Compartment Expansion in *daf-6* Mutants

In addition to actin, our two-hybrid studies suggested that the LIT-1 C-terminal domain can also bind to the proline-rich region of WSP-1, the *C. elegans* homolog of the Wiskott-Aldrich Syndrome Protein (WASP) (Table S2, Figure 7A). Furthermore, we could immunoprecipitate the LIT-1 C-terminal domain using WSP-1 from cultured *Drosophila* S2 cells co-expressing both proteins (Figure 7H), suggesting that LIT-1 and WSP-1 can interact. Although GFP::WSP-1 expressed in amphid sheath glia is diffusely localized (unpublished data), co-expression with mCherry::LIT-1 revealed partial co-localization (Figure 7E–G), supporting the notion that LIT-1 and WSP-1 may interact in vivo.

To determine whether *wsp-1* plays a role in amphid morphogenesis, we examined *wsp-1*(*gm324*) mutants, which, unlike actin mutants, are viable [38]. We did not find any defects in dye filling in the single mutant. However, *wsp-1*(*gm324*) suppresses the *daf-6*(*n1543*) dye-filling defects (Figure 7I). Furthermore, *daf-6* mutants homozygous for both *lit-1*(*ns132*) and *wsp-1*(*gm324*) were as dye-filling defective as *lit-1*(*ns132*); *daf-6*(*n1543*) mutants alone, consistent with the hypothesis that LIT-1 and WSP-1 act in the same pathway.

Interestingly, we found that overexpression of a GFP::LIT-1 fusion protein results in abnormal glial morphology (Figure S5B, compare to Figure S5A) and distorted sensory compartment morphology (Figure S5C, compare to Figure 6A). This result, together with the genetic and physical interactions between LIT-1 and actin and LIT-1 and WASP, are consistent with the possibility that LIT-1 facilitates glial morphogenesis by regulating actin dynamics.

Discussion

lit-1 Regulates the Morphogenesis of a Subcellular Structure

LIT-1 is the *C. elegans* homolog of Nemo-like kinase (NLK) [39], a Serine/Threonine kinase originally described in *Drosophila* [40]. In *C. elegans*, *lit-1* (loss of intestine) was first identified for its role in endoderm specification during early embryogenesis [26]. Subsequent work established *lit-1* as a component of the Wnt/β-catenin asymmetry pathway that directs many cell fate decisions in *C. elegans* [28,29]. NLK also plays roles in control of the Wnt [41,42], TGFβ [43], and Notch [44] signaling pathways in vertebrates.

Although LIT-1/NLK has been implicated in cell fate determination, we identified *lit-1* mutations as suppressors of lesions in *daf-6*, a gene that affects morphogenesis of the amphid glial sensory compartment, but not glial cell fate. Indeed, *lit-1* single mutants seem to have well-specified amphid components.

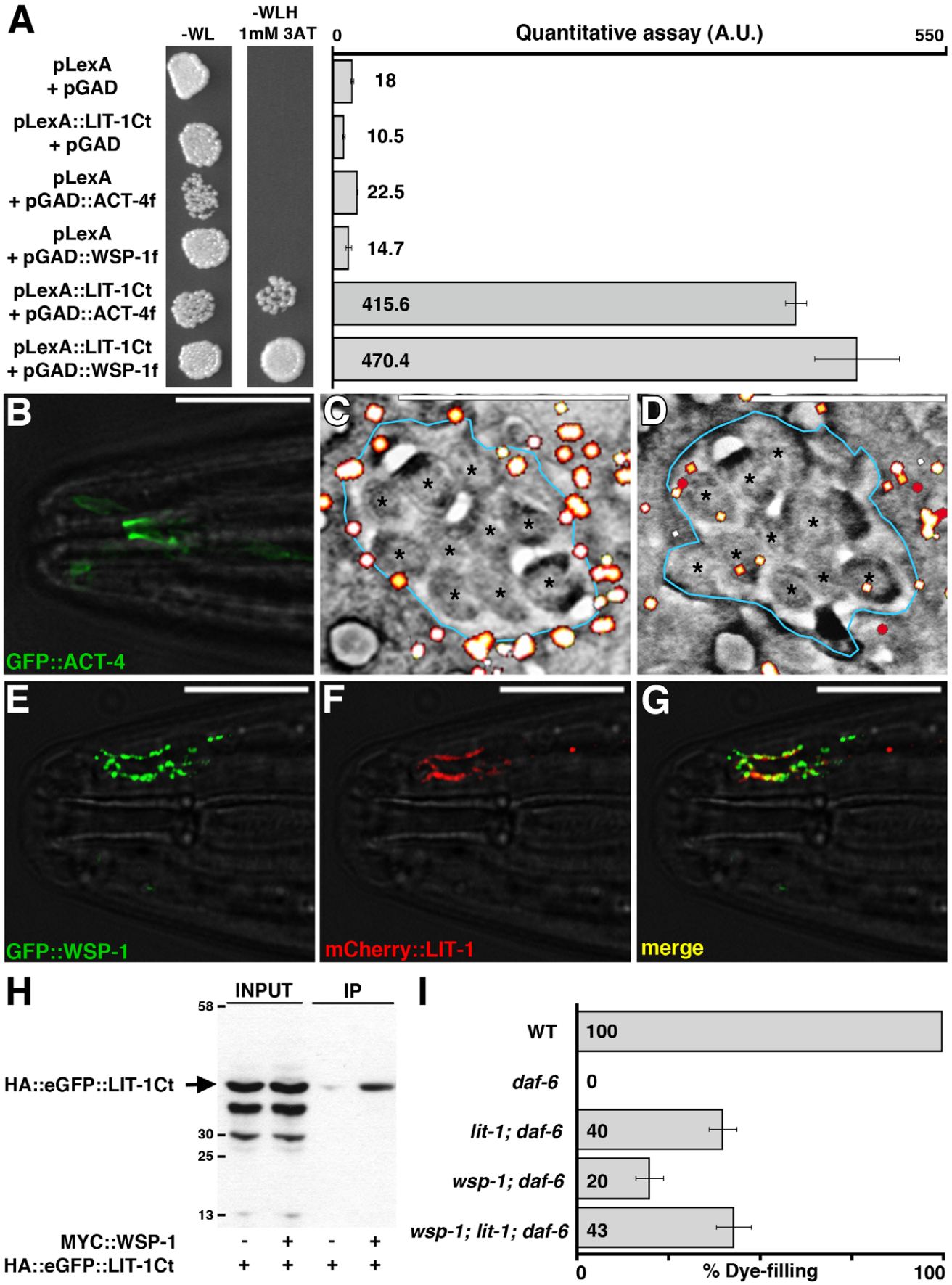
A
-WL
-WLH
1mM 3AT
pLexA
+ pGAD
pLexA::LIT-1Ct
+ pGAD
pLexA
+ pGAD::ACT-4f
pLexA
+ pGAD::WSP-1f
pLexA::LIT-1Ct
+ pGAD::ACT-4f
pLexA::LIT-1Ct
+ pGAD::WSP-1f
0
Quantitative assay (A.U.)
550
18
10.5
22.5
14.7
415.6
470.4
B
GFP::ACT-4
C
D
E
GFP::WSP-1
F
mCherry::LIT-1
G
merge
H
INPUT
IP
58
30
25
13
HA::eGFP::LIT-1Ct
MYC::WSP-1
HA::eGFP::LIT-1Ct
- + - +
+ + + +
I
WT
100
daf-6
0
lit-1; daf-6
40
wsp-1; daf-6
20
wsp-1; lit-1; daf-6
43
0
% Dye-filling
100

Figure 7. The actin cytoskeleton is involved in amphid sensory compartment morphogenesis. (A) Growth assay (left) and quantitative β-galactosidase enzymatic activity assay (right) demonstrating the interaction between LexA fused to the LIT-1 carboxy-terminal domain and GAD fused to fragments of ACT-4 or WSP-1. Error bars, standard deviation. f, fragment. −WL, medium without Tryptophan and Leucine. –WLH, medium without Tryptophan, Leucine, and Histidine. 3AT, 3-amino-1,2,4-triazole. A.U., arbitrary units. (B) Amphid channel localization of GFP::ACT-4 (transgene *nsEx2876*). Anterior is to the left. Scale bar, 10 μm. (C, D) fEM (see Experimental Procedures) of a cross-section through the amphid channel (blue trace) just below the socket-sheath junction (C) or 2 μm posterior (D). White puncta indicate mEos::ACT-4 localization. Transgene used *nsEx2970*. Asterisks, cilia. Scale bars, 1 μm. (E–G) Co-localization of GFP::WSP-1 and mCherry::LIT-1 at the amphid sensory compartment (transgene *nsEx3245*). The *T02B11.3* amphid sheath promoter [32] was used to drive all constructs. Anterior is to the left. Scale bars, 10 μm. (H) The carboxy-terminal domain of LIT-1 co-immunoprecipitates with WSP-1. *Drosophila* S2 cells were transfected with HA::eGFP::LIT-1Ct and with or without MYC::WSP-1. Cell lysates were immunoprecipitated using anti-MYC-conjugated agarose beads and analyzed by anti-HA immunoblot. (I) Dye filling in animals of the indicated genotypes ($n \geq 90$). The alleles used are: *daf-6*(*n1543*), *lit-1*(*ns132*), *wsp-1*(*gm324*). *daf-6* is marked with *unc-3*(*e151*) in all strains. *unc-3*(*e151*) does not affect dye filling (unpublished data). Error bars, SEM. See also Table S2.
doi:10.1371/journal.pbio.1001121.g007

Furthermore, despite an established connection between *lit-1* and the Wnt/β-catenin asymmetry pathway (a major regulator of cell fate decisions in *C. elegans*), we found no evidence linking Wnt signaling to amphid morphogenesis (Table S1). These observations are consistent with the idea that the role of *lit-1* in sensory organ morphogenesis does not involve cell fate decisions, but instead reflects a novel function in cellular morphogenesis.

Within the context of cell fate decisions, LIT-1/NLK often acts by impinging upon the activity of nuclear transcription factors [30,43,44]. It is unclear whether the role of *lit-1* in sensory organ morphogenesis might also involve transcriptional regulation. The C-terminal domain of LIT-1 is required for its role in amphid morphogenesis and for its amphid channel localization, but it is not essential for the ability of LIT-1 to enter the nucleus. This suggests that LIT-1 may exert its primary influence on channel morphogenesis at the channel itself. However, LIT-1 C-terminus can interact not only with cytoskeletal proteins (actin and WASP) but also with the transcription factors ZTF-16 and MEP-1 (Table S2). Thus, while it is likely that sensory compartment localization is important for LIT-1 function, we cannot rule out the possibility that LIT-1 has independent relevant functions in the nucleus.

Opposing Activities of *lit-1* and *daf-6* Direct Sensory Compartment Morphogenesis

Our results suggest that *daf-6* and *lit-1* direct the morphogenesis of the sheath glia sensory compartment by exerting opposing influences. In *daf-6* mutants, neurons and glia form an amphid primordium in which all components are initially linked and aligned; however, the sensory compartment expands abnormally. Conversely, in *lit-1* mutants, the sensory compartment is too narrow. Mutations in *lit-1* can correct for the loss of *daf-6*; thus, *lit-1*; *daf-6* double mutants have relatively normal glial channels. A situation that mimics *lit-1*; *daf-6* double mutants arises in animals with mutations in genes controlling neuronal cilia development. In these animals, channel localization of LIT-1, as well as DAF-6, is perturbed. Consistent with the *lit-1*; *daf-6* phenotype, channel formation is only mildly defective in these mutants [14].

The observation that *lit-1* loss-of-function mutations suppress *daf-6* null alleles argues that *lit-1* cannot function solely upstream of *daf-6* in a linear pathway leading to channel formation. Our data, however, are consistent with the possibility that *daf-6* functions upstream of *lit-1* to inhibit *lit-1* activity. Alternatively, *lit-1* and *daf-6* may act in parallel. Our studies do not currently allow us to distinguish between these models.

Vesicles, the Actin Cytoskeleton, and Sensory Compartment Morphogenesis

How might DAF-6 restrict the size of glial sensory compartments? Electron micrographs of the *C. elegans* amphid reveal the presence of highly organized Golgi stacks near the amphid channel. These images also show vesicles, containing extracellular matrix, that appear to be released by the sheath glia into the channel (Figure 1A) [11]. These studies suggest that vesicular secretion may play a role in channel morphogenesis. Interestingly, DAF-6 is related to Patched, a protein implicated in endocytosis of the Hedgehog ligand, and the *C. elegans* Patched gene *ptc-1* is proposed to regulate vesicle dynamics during germ-cell cytokinesis [45]. Furthermore, DAF-6 can be seen in punctate structures, which may be vesicles [14], and DAF-6 and CHE-14/Dispatched function together in tubulogenesis [14,16], a process hypothesized to require specialized vesicular transport. Together these observations raise the possibility that DAF-6 may restrict amphid sensory compartment expansion by regulating vesicle dynamics in the sheath glia [14].

If indeed DAF-6 controls membrane dynamics, it is possible that LIT-1, which localizes to and functions at the sheath glia channel, also interfaces with such processes. How might LIT-1 localize to the glial sensory compartment and control vesicle dynamics? Previous studies suggest that cortical localization of LIT-1 requires it to stably interact with WRM-1/β-catenin [33,34]. In the sheath glia, however, we found that *wrm-1* is not required for sensory compartment morphogenesis or for LIT-1 localization and that LIT-1 and WRM-1 do not co-localize to the amphid sensory compartment (unpublished data). Instead, we found that LIT-1 physically interacts with actin and that actin is highly enriched around the amphid sensory compartment. Thus, actin might serve as a docking site for LIT-1. The interaction between LIT-1 and actin may not be passive. Indeed, we showed that LIT-1 also binds to WASP, and mutations in *wsp-1*/WASP suppress *daf-6* similarly to mutations in *lit-1*. Furthermore, WASP activity is stimulated by phosphorylation of Serines 483 and 484 [46], suggesting that LIT-1, a Ser/Thr kinase, could activate WASP to promote actin remodeling.

Remodeling of the cortical actin cytoskeleton plays important roles in several aspects of membrane dynamics [47]. For example, WASP-dependent actin polymerization has a well-established role in promoting vesicle assembly during clathrin-mediated endocytosis [48]. Recent work has demonstrated positive roles for actin polymerization in exocytosis as well [49,50]. In pancreatic acinar cells, secretory granules become coated with actin prior to membrane fusion [51], and in neuroendocrine cells, actin polymerization driven by WASP stimulates secretion [52]. During *Drosophila* myoblast fusion, actin polymerization, dependent on WASP and WASP interacting protein (WIP), is required for targeted exocytosis of prefusion vesicles [53], and antibodies against WASP inhibit fusion of purified yeast vacuoles [54]. An attractive possibility, therefore, is that LIT-1 might regulate sensory compartment morphogenesis by altering vesicle trafficking through WASP-dependent actin polymerization.

Glial ensheathment is a feature of many animal sensory organs and synapses, and LIT-1 and WASP are highly conserved, suggesting that our studies may be broadly relevant. Interestingly,

LIT-1 was recently shown to be required for cell invasion through basement membranes in *C. elegans* and in metastatic carcinoma cells [55], processes that require extensive remodeling of the actin cytoskeleton. Our results may, thus, represent a general mechanism for regulating cell shape changes using localized interactions of LIT-1/NLK with cytoskeletal proteins.

Materials and Methods

Strains, Plasmid Construction, and *lit-1* Mapping and Cloning

See Supporting Information.

Dye-Filling Assay

Animals were washed off NGM plates with M9 buffer, resuspended in a solution of 10 µg/mL of DiI (1,1′-dioctadecyl-3,3,3′,3′-tetramethylindocarbocyanine perchlorate) (Invitrogen D282), and rotated in the dark for 1.5 h at room temperature. Animals were then transferred to a fresh NGM plate, anaesthetized with 20 mM sodium azide, and observed using a dissecting microscope equipped with epifluorescence. Animals in which none of the amphid neurons filled with dye were scored as dye-filling defective (Dyf). For the sensitized dye-filling assay, 1 µg/mL of DiI was used, and the incubation time was 15 min. Animals were scored as dye filling defective (Dyf) if either one or two amphids failed to fill.

Transmission Electron Microscopy and Fluorescence Electron Microscopy (fEM)

See Supporting Information and [37].

Fluorescence Microscopy and Image Analysis

Images were acquired using a DeltaVision Image Restoration Microscope (Applied Precision) equipped with a 60×/NA 1.42 Plan Apo N oil immersion objective (Olympus) and a Photometrics CoolSnap camera (Roper Scientific), or an Upright Axioplan LSM 510 laser scanning confocal microscope (Zeiss) equipped with a C-Apochromat 40×/NA 1.2 objective. Acquisition, deconvolution, and analysis of images from the DeltaVision system were performed with Softworx (Applied Precision); images from the confocal microscope were acquired and analyzed using LSM 510 (Zeiss).

Yeast Two-Hybrid Screen

LexA::LIT-1Ct was used as bait in a Y2H screen using the DUALHhybrid kit (Dualsystems Biotech) in conjunction with the *C. elegans* Y2H cDNA library (Dualsystems Biotech), as described by the manufacturer. For the growth assay, cultures growing on Synthetic Complete Dextrose –Tryptophan, –Leucine (SCD –WL) plates were resuspended in water to $OD_{660} = 0.1$. 5 µL of each culture were seeded on SCD –WL plates and SCD –WL, –Histidine (H) plates + 1 mM 3AT (3-amino-1,2,4-triazole) to select for HIS3 expression. β-galactosidase assay was performed using the yeast β-galactosidase assay kit (Thermo Scientific).

Protein Interaction Studies

Drosophila S2 cells (Invitrogen) cultured at 25°C were transfected with FuGene HD (Roche), incubated for 3 d, and lysed in 1 mL of IP buffer (60 mM Tris HCl, pH 8.0, 1% Tergitol type NP-40 (Sigma), 10% glycerol, 1×Complete protease inhibitor cocktail (Roche), 1×PhoStop phosphatase inhibitor cocktail (Roche)). 100 µL of lysate was stored on ice as input. Immunoprecipitation was performed with the remaining lysate for 2 h at 4°C, using goat anti-myc-conjugated agarose beads (Genetex). Immunoprecipitated complexes were released from the beads with 100 µL of sample buffer (same as IP buffer with the addition of 2% sodium dodecylsulfate (SDS), 0.1 M Dithiothreitol (DTT), and 0.01% bromophenol blue). Samples were analyzed on NuPage 4%–12% Bis-Tris gels (Invitrogen). Immunoblotting was performed using rat monoclonal anti-HA 3F10 coupled to horseradish peroxidase (HRP) (Roche), 1:2,000; rabbit polyclonal anti-myc (AbCam), 1:5,000; And goat polyclonal anti-rabbit (Pierce) coupled to HRP, 1:2,000.

Supporting Information

Figure S1 Amphid sensory compartment morphogenesis in wild-type embryos. Electron micrographs of cross-sections through the amphid primordium in wild-type animals. Top: At approximately 380 min after fertilization, the amphid pocket is blocked anteriorly by a cap formed by the sheath glia (left). More posteriorly (middle and right), the sheath wraps around the dendrites of the amphid neurons. Bottom: At approximately 400 min after fertilization, the amphid channel is open, with filaments (asterisk) visible at the level of the socket (left; arrow indicates socket self junction). More posteriorly (middle and right), the sheath glia wraps around the dendrites of the amphid neurons. Filaments (asterisk) can be seen in the middle section.
(TIF)

Figure S2 Dye-filling assay and *lit-1(ns132)* mapping and cloning. (A–C) Fluorescence images of (A) wt, (B) *daf-6(e1377)*, and (C) *lit-1(ns132)*; *daf-6(e1377)* animals after incubation for 1.5 h in 10 µg/mL of DiI (red). Scale bars, 50 µm. (D) Using SNP mapping (see Supplemental Materials and Methods, Text S1), *ns132* was mapped to the right end of chromosome III, distal to the SNP F54F12:17329 at genetic position +20.72. The cosmids ZK520, ZK525, W96F12, and K08E3 were used for the construction of transgenic strains (see panel E). (E) Dye-filling in animals of the indicated genotypes ($n \geq 90$). The alleles used were *daf-6(e1377)* and *lit-1(ns132)*. *lit-1* genomic and *lit-1(ns132)* genomic correspond to constructs pGO1 and pGO2, respectively (see Supplemental Materials and Methods, Text S1).
(TIF)

Figure S3 Nuclear localization of LIT-1 is not abrogated by disruption of the LIT-1 carboxy-terminal domain. (A–C) Fluorescence images of sheath glia cell body and nucleus in animals transgenic for the indicated GFP::LIT-1 fusion protein. Transgenes depicted: *nsEx2606* (A), *nsEx2609* (B), *nsEx2747* (C). Arrow, cell nucleus. Scale bar, 10 µm. The *T02B11.3* promoter was used to drive all constructs.
(TIF)

Figure S4 Sensory compartment localization of LIT-1, MOM-4, and ACT-4 are independent of *daf-6*. (A–C) Fluorescence images of adult *daf-6(n1543)* animals expressing the indicated GFP fusion proteins. The *T02B11.3* amphid sheath promoter was used to drive all constructs. Trangenes depicted: *nsEx2606* (A), *nsEx2840* (B), *nsEx2876* (C). Anterior is to the left. Scale bars, 10 µm.
(TIF)

Figure S5 Overexpression of LIT-1 within the sheath glia disrupts cellular morphology. (A) Fluorescence projection image of the sheath glia promoter *F16F9.3* driving dsRed (transgene *nsEx3272*). (B) Fluorescence projection image of a transgenic animal carrying a high copy number of the *T02B11.3* amphid sheath promoter driving GFP::LIT-1 (transgene *nsEx2619*). Compare the extensive branching of the sheath glia process with

(B). (C) Fluorescence image of the sensory compartment of an animal with the same genotype as the one in (B). Compare with Figure 6A. Anterior is to the left. Scale bars, 10 μm.
(TIF)

Table S1 Components of the Wnt signaling pathway do not affect amphid morphogenesis.
(DOC)

Table S2 Clones identified from a yeast-two-hybrid screen for proteins that interact with the carboxy-terminal domain of LIT-1.
(DOC)

Text S1 Supplemental Materials and Methods.
(DOC)

Acknowledgments

We thank Craig Mello and Cori Bargmann for strains, Yuji Kohara for cDNA clones, the Sanger Center for cosmids, Maya Tevlin for sharing microarray data, Max Heiman for advice on imaging, Catherine Oikonomou and Fred Cross for help with yeast techniques, and members of the Shaham lab for comments on the manuscript. Some nematode strains used in this work were provided by the *Caenorhabditis* Genetics Center, which is funded by the NIH National Center for Research Resources (NCRR).

Author Contributions

The author(s) have made the following declarations about their contributions: Conceived and designed the experiments: GO EAP EMJ SS. Performed the experiments: GO EAP SW YL. Analyzed the data: GO EAP SW EMJ SS.

References

1. Burkitt GH, Young B, Heath JW (1993) Wheater's functional histology: a text and colour atlas. New York: Churchill Livinstone.
2. Ross MH, Romrell LJ, Kaye GI (1995) Histology: a text and atlas. Baltimore: Williams & Wilkins.
3. Bell J, Bolanowski S, Holmes MH (1994) The structure and function of Pacinian corpuscles: a review. Prog Neurobiol 42: 79–128.
4. Suzuki Y, Takeda M, Farbman AI (1996) Supporting cells as phagocytes in the olfactory epithelium after bulbectomy. J Comp Neurol 376: 509–517.
5. Hansel DE, Eipper BA, Ronnett GV (2001) Neuropeptide Y functions as a neuroproliferative factor. Nature 410: 940–944.
6. Rio C, Dikkes P, Liberman MC, Corfas G (2002) Glial fibrillary acidic protein expression and promoter activity in the inner ear of developing and adult mice. J Comp Neurol 442: 156–162.
7. Young RW, Bok D (1969) Participation of the retinal pigment epithelium in the rod outer segment renewal process. J Cell Biol 42: 392–403.
8. Bacaj T, Tevlin M, Lu Y, Shaham S (2008) Glia are essential for sensory organ function in C. elegans. Science 322: 744–747.
9. Spacek J (1985) Three-dimensional analysis of dendritic spines. III. Glial sheath. Anat Embryol 171: 245–252.
10. Ventura R, Harris KM (1999) Three-dimensional relationships between hippocampal synapses and astrocytes. J Neurosci 19: 6897–6906.
11. Ward S, Thomson N, White JG, Brenner S (1975) Electron microscopical reconstruction of the anterior sensory anatomy of the nematode Caenorhabditis elegans. J Comp Neurol 160: 313–337.
12. Albert PS, Brown SJ, Riddle DL (1981) Sensory control of dauer larva formation in Caenorhabditis elegans. J Comp Neurol 198: 435–451.
13. Perkins LA, Hedgecock EM, Thomson JN, Culotti JG (1986) Mutant sensory cilia in the nematode Caenorhabditis elegans. Dev Biol 117: 456–487.
14. Perens EA, Shaham S (2005) C. elegans daf-6 encodes a patched-related protein required for lumen formation. Dev Cell 8: 893–906.
15. Herman RK (1987) Mosaic analysis of two genes that affect nervous system structure in Caenorhabditis elegans. Genetics 116: 377–388.
16. Michaux G, Gansmuller A, Hindelang C, Labouesse M (2000) CHE-14, a protein with a sterol-sensing domain, is required for apical sorting in C. elegans ectodermal epithelial cells. Curr Biol 10: 1098–1107.
17. Rocheleau CE, Yasuda J, Shin TH, Lin R, Sawa H, et al. (1999) WRM-1 activates the LIT-1 protein kinase to transduce anterior/posterior polarity signals in C. elegans. Cell 97: 717–726.
18. Symons M, Derry JM, Karlak B, Jiang S, Lemahieu V, et al. (1996) Wiskott-Aldrich syndrome protein, a novel effector for the GTPase CDC42Hs, is implicated in actin polymerization. Cell 84: 723–734.
19. Sulston JE, Schierenberg E, White JG, Thomson JN (1983) The embryonic cell lineage of the nematode Caenorhabditis elegans. Dev Biol 100: 64–119.
20. Heiman MG, Shaham S (2009) DEX-1 and DYF-7 establish sensory dendrite length by anchoring dendritic tips during cell migration. Cell 137: 344–355.
21. Cassada RC, Russell RL (1975) The dauerlarva, a post-embryonic developmental variant of the nematode Caenorhabditis elegans. Dev Biol 46: 326–342.
22. Riddle DL, Swanson MM, Albert PS (1981) Interacting genes in nematode dauer larva formation. Nature 290: 668–671.
23. Starich TA, Herman RK, Kari CK, Yeh WH, Schackwitz WS, et al. (1995) Mutations affecting the chemosensory neurons of Caenorhabditis elegans. Genetics 139: 171–188.
24. Yoshimura S, Murray JI, Lu Y, Waterston RH, Shaham S (2008) mls-2 and vab-3 Control glia development, hlh-17/Olig expression and glia-dependent neurite extension in C. elegans. Development 135: 2263–2275.
25. Landmann F, Quintin S, Labouesse M (2004) Multiple regulatory elements with spatially and temporally distinct activities control the expression of the epithelial differentiation gene lin-26 in C. elegans. Dev Biol 265: 478–490.
26. Kaletta T, Schnabel H, Schnabel R (1997) Binary specification of the embryonic lineage in Caenorhabditis elegans. Nature 390: 294–298.
27. Shin TH, Yasuda J, Rocheleau CE, Lin R, Soto M, et al. (1999) MOM-4, a MAP kinase kinase kinase-related protein, activates WRM-1/LIT-1 kinase to transduce anterior/posterior polarity signals in C. elegans. Mol Cell 4: 275–280.
28. Mizumoto K, Sawa H (2007) Two betas or not two betas: regulation of asymmetric division by beta-catenin. Trends Cell Biol 17: 465–473.
29. Phillips BT, Kimble J (2009) A new look at TCF and beta-catenin through the lens of a divergent C. elegans Wnt pathway. Dev Cell 17: 27–34.
30. Lo MC, Gay F, Odom R, Shi Y, Lin R (2004) Phosphorylation by the beta-catenin/MAPK complex promotes 14-3-3-mediated nuclear export of TCF/POP-1 in signal-responsive cells in C. elegans. Cell 117: 95–106.
31. Kidd AR, Miskowski JA, Siegfried KR, Sawa H, Kimble J (2005) A beta-catenin identified by functional rather than sequence criteria and its role in Wnt/MAPK signaling. Cell 121: 761–772.
32. Wang Y, Apicella A, Lee SK, Ezcurra M, Slone RD, et al. (2008) A glial DEG/ENaC channel functions with neuronal channel DEG-1 to mediate specific sensory functions in C. elegans. EMBO J 27: 2388–2399.
33. Takeshita H, Sawa H (2005) Asymmetric cortical and nuclear localizations of WRM-1/beta-catenin during asymmetric cell division in C. elegans. Genes Dev 19: 1743–1748.
34. Mizumoto K, Sawa H (2007) Cortical beta-catenin and APC regulate asymmetric nuclear beta-catenin localization during asymmetric cell division in C. elegans. Dev Cell 12: 287–299.
35. Drenckhahn D, Mannherz HG (1983) Distribution of actin and the actin-associated proteins myosin, tropomyosin, alpha-actinin, vinculin, and villin in rat and bovine exocrine glands. Eur J Cell Biol 30: 167–176.
36. Lee RW, Trifaró JM (1981) Characterization of anti-actin antibodies and their use in immunocytochemical studies on the localization of actin in adrenal chromaffin cells in culture. Neuroscience 6: 2087–2108.
37. Watanabe S, Punge A, Hollopeter G, Willig KI, Hobson RJ, et al. (2011) Protein localization in electron micrographs using fluorescence nanoscopy. Nat Methods 8: 80–84.
38. Withee J, Galligan B, Hawkins N, Garriga G (2004) Caenorhabditis elegans WASP and Ena/VASP proteins play compensatory roles in morphogenesis and neuronal cell migration. Genetics 167: 1165.
39. Brott BK, Pinsky BA, Erikson RL (1998) Nlk is a murine protein kinase related to Erk/MAP kinases and localized in the nucleus. Proc Natl Acad Sci U S A 95: 963–968.
40. Choi KW, Benzer S (1994) Rotation of photoreceptor clusters in the developing Drosophila eye requires the nemo gene. Cell 78: 125–136.
41. Ishitani T, Ninomiya-Tsuji J, Nagai S, Nishita M, Meneghini M, et al. (1999) The TAK1-NLK-MAPK-related pathway antagonizes signalling between beta-catenin and transcription factor TCF. Nature 399: 798–802.
42. Thorpe CJ, Moon RT (2004) nemo-like kinase is an essential co-activator of Wnt signaling during early zebrafish development. Development 131: 2899–2909.
43. Ohkawara B, Shirakabe K, Hyodo-Miura J, Matsuo R, Ueno N, et al. (2004) Role of the TAK1-NLK-STAT3 pathway in TGF-beta-mediated mesoderm induction. Genes Dev 18: 381–386.
44. Ishitani T, Hirao T, Suzuki M, Isoda M, Ishitani S, et al. (2010) Nemo-like kinase suppresses Notch signalling by interfering with formation of the Notch active transcriptional complex. Nat Cell Biol 12: 278–285.
45. Kuwabara PE, Lee MH, Schedl T, Jefferis GS (2000) A C. elegans patched gene, ptc-1, functions in germ-line cytokinesis. Genes Dev 14: 1933–1944.
46. Cory GO, Cramer R, Blanchoin L, Ridley AJ (2003) Phosphorylation of the WASP-VCA domain increases its affinity for the Arp2/3 complex and enhances actin polymerization by WASP. Mol Cell 11: 1229–1239.
47. Lanzetti L (2007) Actin in membrane trafficking. Curr Opin Cell Biol 19: 453–458.
48. Galletta BJ, Mooren OL, Cooper JA (2010) Actin dynamics and endocytosis in yeast and mammals. Curr Opin Biotechnol 21: 604–610.
49. Malacombe M, Bader MF, Gasman S (2006) Exocytosis in neuroendocrine cells: new tasks for actin. Biochim Biophys Acta 1763: 1175–1183.

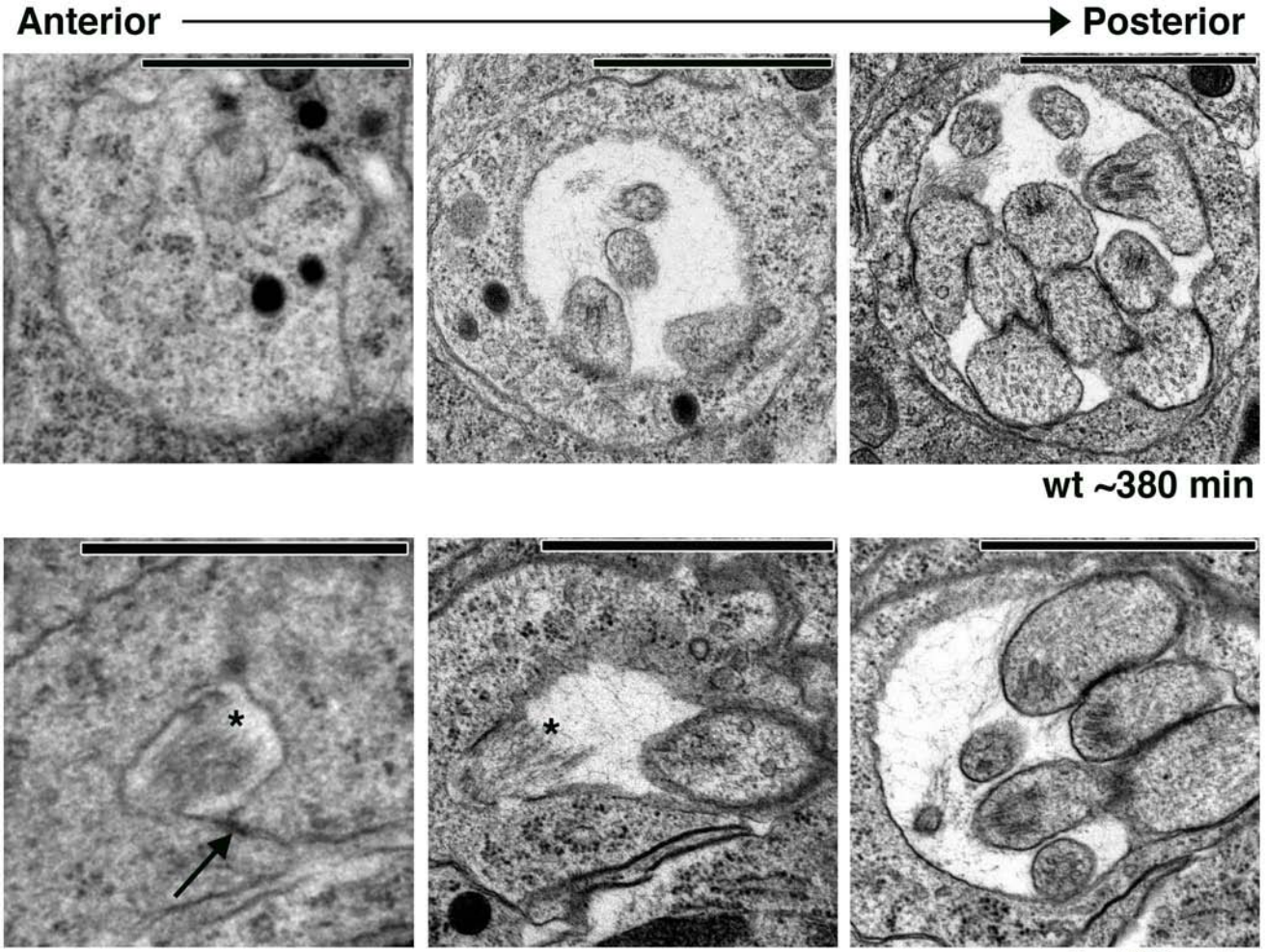
Anterior
Posterior
wt ~380 min
wt ~400 min

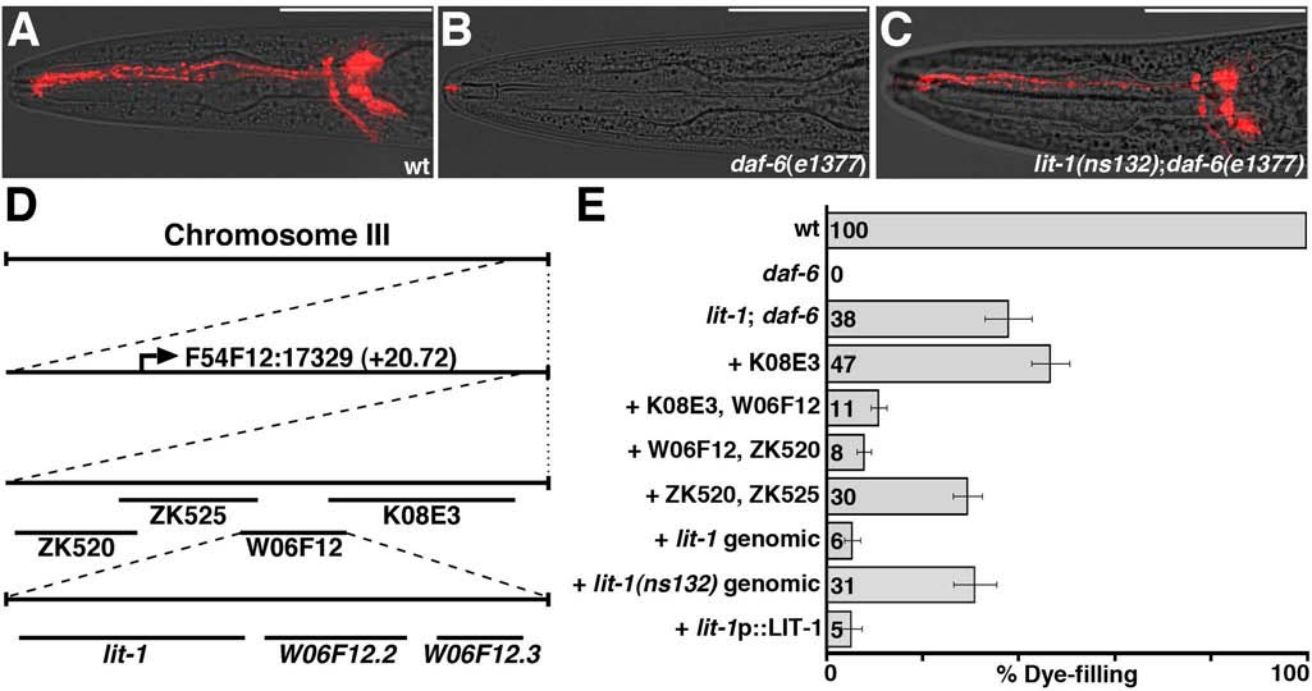
A
wt
B
daf-6(e1377)
C
lit-1(ns132);daf-6(e1377)
D
Chromosome III
F54F12:17329 (+20.72)
ZK525
K08E3
ZK520
W06F12
lit-1
W06F12.2
W06F12.3
E
wt 100
daf-6 0
lit-1; daf-6 38
+ K08E3 47
+ K08E3, W06F12 11
+ W06F12, ZK520 8
+ ZK520, ZK525 30
+ lit-1 genomic 6
+ lit-1(ns132) genomic 31
+ lit-1p::LIT-1 5
0
% Dye-filling
100

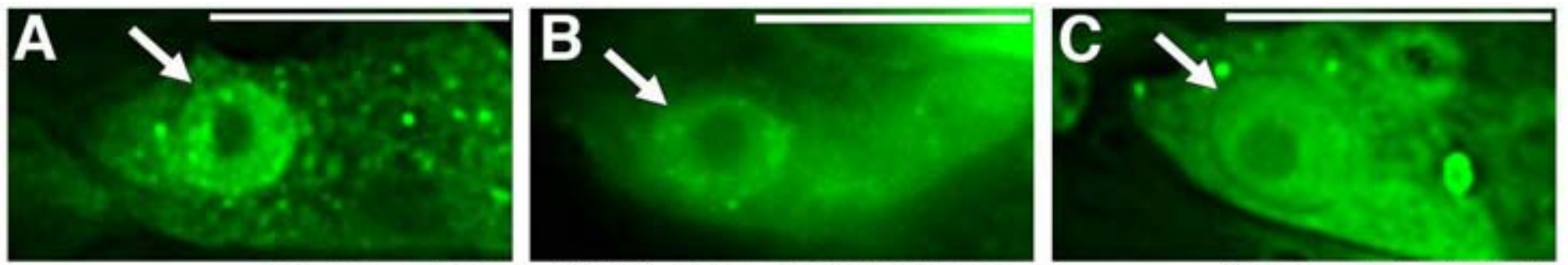
A
B
C
GFP::LIT-1
GFP::LIT-1Q437Stop
GFP::LIT-1ΔCt

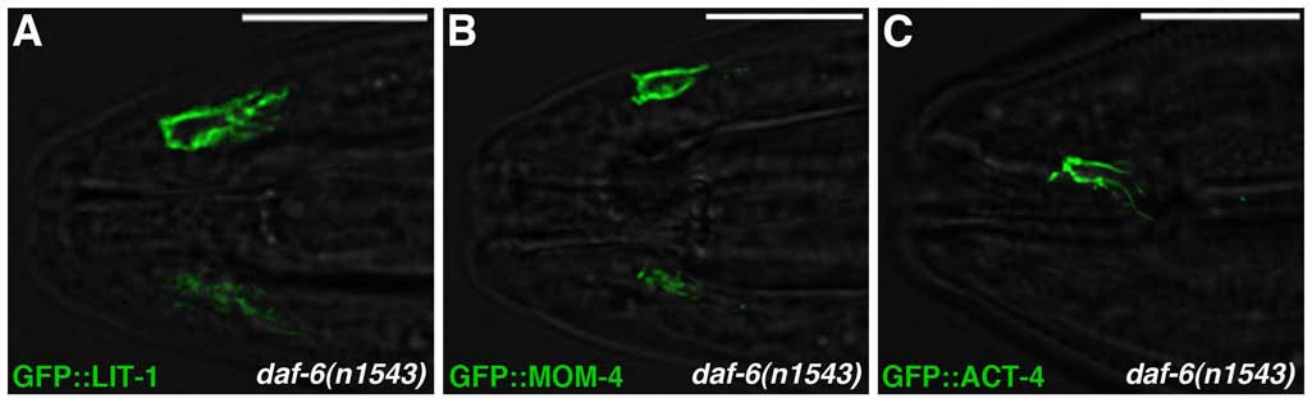
A
GFP::LIT-1
daf-6(n1543)
B
GFP::MOM-4
daf-6(n1543)
C
GFP::ACT-4
daf-6(n1543)

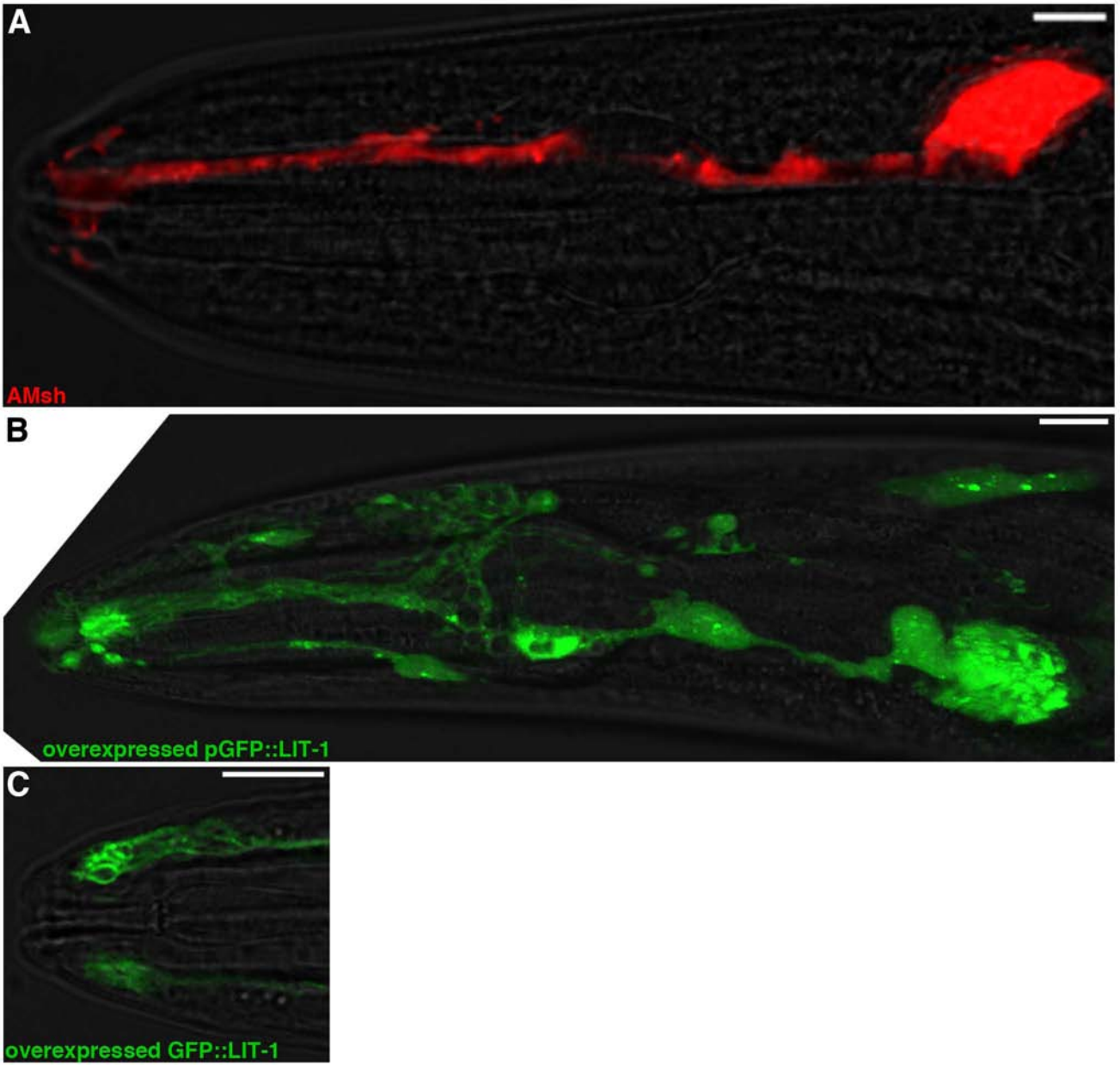
A
AMsh
B
overexpressed pGFP::LIT-1
C
overexpressed GFP::LIT-1

Table S1. Components of the Wnt signaling pathway do not affect amphid morphogenesis

Common name	*C .elegans* gene name	Allele	% Dye-filling[a]	% Dye-filling in *daf-6*(*n1543*)[b]
Porcupine	*mom-1*	RNAi	ND[c]	0
Wntless	*mig-14*	*mu71*	100	5
		ga62	100	2
Wnt	*lin-44*	*n1792*	100	0
	egl-20	*mu27*[d]	100	0
	cwn-1	*ok546*	100	3
	cwn-2	*ok895*	100	0
	mom-2	*ne834*	100	0
		or309	100	ND
Frizzled	*lin-17*	*n671*	100	4
		n698	100	ND
		n3091	100	ND
	mig-1	*e1787*	100	6
	mom-5	*or57, zu193*	100	ND
		RNAi	ND	0
	cfz-2	*ok1201*	100	5
	mig-1 lin-17; cfz-2	*e1787, n677, ok1201* respectively	100	0
Dishevelled	*mig-5*	*rh147*	100	0
	dsh-1	*ok1445*	100	0
		RNAi	ND	0
	dsh-2	*ok2162*	100	ND
		RNAi	ND	0
Ryk	*lin-18*	*e620*	100	0
β-catenin	*bar-1*	*ga80*	100	2
	wrm-1	*ne1982*	100	1
	hmp-2	RNAi	ND	0
	sys-1	*q544*	100	ND
		RNAi	ND	0
TCF/LEF	*pop-1*	*q624*	100	0
		RNAi	ND	0
ROR1	*cam-1*	*ks52*	100	8
Van Gogh/ Strabismus	*vang-1*	*ok1142*	100	0

[a] n≥100 for each genotype.

[b] Full genetic background was *unc-3*(*e151*) *daf-6*(*n1543*) except for RNAi experiments where background was *rrf-3*(*pk1426*); *unc-3*(*e151*)*daf-6*(*n1543*). *rrf-3* increases the sensitivity to RNAi [1], but does not affect dye-filling (data not shown); n≥100 for all experiments.

[c] ND, not determined.
[d] The reference *egl-20* allele *n585* harbors a background mutation that suppresses the dye-filling defects of *daf-6*(*n1543*). The *mu27* allele, shown here, has the same molecular lesion as *n585* [2], but does not suppress *daf-6*.

1. Simmer F, Tijsterman M, Parrish S, Koushika SP, Nonet ML et al. (2002) Loss of the putative RNA-directed RNA polymerase RRF-3 makes C. elegans hypersensitive to RNAi. Curr Biol 12: 1317-1319.

2. Maloof JN, Whangbo J, Harris JM, Jongeward GD, Kenyon C (1999) A Wnt signaling pathway controls hox gene expression and neuroblast migration in C. elegans. Development 126: 37-49.

Table S2. Clones identified from a yeast-two-hybrid screen for proteins that interact with the carboxy-terminal domain of LIT-1

Gene	No. clones found	Description
mep-1	1	zinc-finger protein
T24E12.9	1	protein of unknown function
vit-3	2	vitellogenin
fbp-1	1	fructose 1,6-bisphosphatase
act-4	4	actin
Y87G2A.1	2	protein of unknown function
wsp-1	1	WASP
ztf-16	1	zinc-finger protein
C50F4.1	1	protein of unknown function
C44B12.5	6	protein of unknown function
nrde-3	1	argonaute protein
ost-1	1	osteonectin, ECM protein
unc-52	1	perlecan, ECM protein
tag-30	1	protein of unknown function
vit-4	1	vitellogenin
C34F11.3	1	adenosine monophosphate deaminase

Supplemental Materials and Methods

Strains

Strains were handled using standard methods [1]. All strains were maintained and scored at 20°C unless otherwise indicated. The alleles used in this study are: *daf-6*(*e1377*, *n1543*) [2] and [3] respectively), *lit-1*(*t1512*) [4], *lit-1*(*ns132*) (described here), *che-14*(*ok193*) [5], *wsp-1*(*gm324*) [6], *mom-4*(*ne1539*)[7], a gift from Craig Mello), *daf-19*(*m86*) [8], *daf-16*(*mu86*)([9], *mig-14*(mu71) [10], *mig-14*(*ga62*)[11], *lin-44*(*n1792*) [12], *egl-20*(*n585*, *mu27*) [13] and [10] respectively), *cwn-1*(*ok546*) [14], *cwn-2*(*ok895*) [14], *mom-2*(*ne834*) [7], a gift from Craig Mello), *mom-2*(*or309*) [15], *lin-17*(*n671*, *n698*) [16], *lin-17*(*n3091*) [17], *mig-1*(*e1787*) [18], *mom-5*(*or57*) [15], *mom-5*(*zu193*) [19], *cfz-2*(*ok1201*) [14], *mig-5*(*rh147*) [20], *lin-18*(*e620*) [16], *bar-1*(*ga80*)) [11], *wrm-1*(*ne1982*) [7], a gift from Craig Mello), *pop-1*(*q624*) [21], *cam-1*(*ks52*) [22], *vang-1*(*ok1142*) [23], *unc*-3(*e151*) [24], *unc-32*(*e189*) [25].

Unstable extrachromosomal transgenes used in this study:

Extrachromosomal array(s)	Constructs
nsEx1933, *nsEx1934*, *nsEx1935, nsEx1936*	pGO1, pMH135
nsEx1931, *nsEx1932*	pGO2, pMH135
nsEx2159, *nsEx2160*	pGO6, *ptr-10*pro::NLSRFP, pRF4
nsEx2078, *nsEx2079*, *nsEx2080*, *nsEx2081*	pGO8, pMH135
nsEx2108, *nsEx2109*, *nsEx2110*, *nsEx2111*, *nsEx2112*, *nsEx2113*	pGO10, *vap-1*pro::GFP
nsEx2308, *nsEx2309*, *nsEx2310*	pGO17, *vap-1*pro::GFP, pRF4
nsEx2952, *nsEx2953*, *nsEx2954*	pGO18, pMH135
nsEx2541, *nsEx2542*, *nsEx2543*	pGO20, pEP51
nsEx2539, *nsEx2540*	pGO32, pEP51
nsEx2605, *nsEx2606*, *nsEx2607*, *nsEx2608, nsEx2619*, *nsEx2829*, *nsEx2830*, *nsEx2831*	pGO38, pRF4
nsEx2609, *nsEx2610*, *nsEx2611*, *nsEx2612*	pGO47, pRF4

nsEx2626, *nsEx2627*, *nsEx2628*, *nsEx2629*,	pGO56, pRF4
nsEx2747, *nsEx2748*, *nsEx2749*	pGO73, pRF4
nsEx2760, *nsEx2761*, *nsEx2762*, *nsEx2766*, *nsEx2767*, *nsEx2768*, *nsEx2750*, *nsEx2751*,*nsEx2752*	*T02B11.3*pro::GFP, *gcy-5*pro::mCherry, pEP51
nsEx2838, *nsEx2839*, *nsEx2840*	pGO91, pRF4
nsEx2874, *nsEx2875*, *nsEx2876*	pGO116, pGO93
nsEx2968, *nsEx2969*, *nsEx2970*	pGO120, pRF4
nsEx3243, *nsEx3244*, *nsEx3245*, *nsEx3246*	pGO177, pGO65, pRF4

Plasmid Construction

Table of the plasmids used in this study. All pGO constructs were made using pPD95.75 (Andrew Fire) as a backbone, unless otherwise noted.

Plasmid	Description	Details
pGO1	*lit-1* genomic region	8.2 kb genomic region that includes the lit-1 locus (W06F12.1b.1 transcript) with a 2.1 kb promoter region and a 637 bp 3'UTR (SalI/AflII) Forward primer: gtcgaccgatttttttcacg Reverse primer: gtgaaagaactcggtagtattggcac
pGO2	*lit-1*(*ns132*) genomic region	Same as pGO1 but amplified from the *lit-1*(*ns132*) strain
pGO6	*lit-1*pro::NLS-GFP	*lit-1*pro consists of 2.5 kb upstream of the *lit-1* start site (W06F12.1b.1 transcript) (SphI/BamHI). Cloned in pPD95.69 (Andrew Fire)
pGO8	*lit-1*pro::LIT-1	*lit-1* cDNA (yk1457b04) a gift from Yuji Kohara (AgeI/EcoRI)
pGO10	*lin-26myo-2*pro::LIT-1	The e1 *lin-26* promoter fragment [26] fused to the *myo-2* minpro [27] (a gift from Maxwell G. Heiman [28] (SphI/XbaI),
pGO17	*lit-1*pro::NLS-RFP	see pGO6
pGO18	*dyf-7*pro::LIT-1	*dyf-7*pro (SphI/XmaI) a gift from Maxwell G. Heiman [28], driving the *lit-1* cDNA (see pGO10)
pGO20	*lin-26myo-2*pro::GFP::LIT-1	*lin-26myo-2*pro (see pGO10) driving a rescuing GFP::LIT-1 fusion
pGO32	*vap-1*pro::GFP::LIT-1	*vap-1*pro a gift from Leo Liu. See also

		[29]
pGO38	*T02B11.3*pro::GFP::LIT-1	*T02B11.3*pro a gift from Maya Tevlin [30]
pGO47	*T02B11.3*pro::GFP::LIT-1Q437Stop	The *lit-1* cDNA truncated at Q437
pGO56	*T02B11.3*pro::GFP::LIT-1Ct	GFP fused to the carboxy-terminal domain of LIT-1 (last 103aa, EEGRLRFH...PPSPQAW)
pGO65	*F16F9.3*pro::mCherry::LIT-1	*F16F9.3*pro a gift from Maya Tevlin [31]
pGO73	*T02B11.3*pro::GFP::LIT-1ΔCt	GFP fused to *lit-1* cDNA truncated at L359
pGO87	pLexA-N::LIT-1Ct	LexA fused to the carboxy-terminal domain of LIT-1 (last 103aa, EEGRLRFH...PPSPQAW)
pGO91	*T02B11.3*pro::GFP::MOM-4	GFP fused to *mom-4* cDNA (yk1072f05), a gift from Yuji Kohara
pGO93	*pha-4*pro::mCherry	*pha-4*pro a gift from Maxwell G. Heiman
pGO116	*T02B11.3*pro::GFP::ACT-4	GFP fused to *act-4* cDNA
pGO119	*Ac*::MYC::WSP-1	myc tagged *wsp-1* cDNA in the pAc, Drosophila actin 5c promoter vector, a gift from Michael Chiorazzi; see [32]
pGO120	T02B11.3pro::mEos::ACT-4	mEos a gift from Loren L Looger. See [33]
pGO123	*Ac::*HA::eGFP::LIT-1	See pGO119. eGFP a gift from Maya Bader
pGO131	*T02B11.3*pro::GFP::ACT-1	*T02B11.3*pro a gift from Maya Tevlin [30]
pGO177	*T02B11.3*pro::GFP::WSP-1	*T02B11.3*pro a gift from Maya Tevlin [30]
pRF4	*rol-6*(*su1006*)	from [34]
pMH135	*pha-4*pro::GFP	a gift from Maxwell G. Heiman [28]
pEP51	*unc-122*pro::GFP	coelomocyte marker
	*ptr-10*pro::NLS-RFP	from [35]
	*vap-1*pro::GFP	*vap-1*pro a gift from Leo Liu. See also [29]
	*gcy-5*pro::mCherry	*gcy-5*pro after [36]
	*T02B11.3*pro::GFP	a gift from Maya Tevlin [30]
	*F16F9.3*pro::mCherry	a gift from Maya Tevlin [31]

lit-1 Mapping and Cloning

ns132 was mapped using single nucleotide polymorphism mapping [37] to the right arm of Chromosome III. We generated transgenic *ns132*; *daf-6(e1377)* animals carrying extrachromosomal arrays of cosmids from this region (provided by the Sanger Center, Cambridge, UK). The genes in the rescuing cosmid, W06F12, were sequenced, and a C->T transition creating a premature stop codon was identified in the last exon of the *lit-1* gene.

Transmission Electron Microscopy (EM)

Previously described conventional fixation methods were used for adult animals [29]. High-pressure fixation was used for embryos and some adult animals. Briefly, samples were frozen using the Leica High Pressure Freezer EM-PACT2 (pressure of 18,000 bar, cooling rate of 20,000 °C/sec). Freeze substitution was performed using the Leica EM AFS2 Automatic Freeze Substitution System [38]. Ultrathin serial sections (60 nm) were cut using a REICHERT Ultra-Cut-E ultramicrotome and collected on Pioloform-coated single-slot copper grids. EM images for every other section were acquired using an FEI Tecnai G2 Spirit BioTwin transmission electron microscope operating at 80 kV with a Gatan 4K x 4K digital camera.

Fluorescence Electron Microscopy (fEM)

Sample preparation: *C. elegans* animals expressing mEos2::ACT-4 [33] were prepared for fEM as previously described [39]. Transgenic animals were raised in the dark and adults were rapidly frozen together with bacteria, as a cryoprotectant,

using a high-pressure freezer (Bal-Tec, HM010). Frozen samples were transferred under liquid nitrogen into cryovials containing 0.1% potassium permanganate (EMS) + 0.001% osmium tetroxide (EMS, crystals) in 95% acetone. Freeze-substitution and subsequent plastic embedding were carried out in an automated freeze-substitution unit as follows: -90°C for 30 h, 5°C/h to -30°C, -30°C for 2 h for the freeze-substitution and -30°C for 48 h for the plastic embedding. Fixatives were washed out with 95% ethanol 6 times over 2 h. Animals were then infiltrated with glycol methacrylate (GMA) solutions in three steps: 30% for 5 h, 70% for 6 h, and 100% overnight. Specimens were moved to a cap of polypropylene BEEM capsules (EBSciences), and the plastic media was exchanged with freshly mixed and pre-cooled GMA three times over a period of 6 h. At the last step of the exchange, animals were separated from the bacteria using tweezers (EMS, #5), and GMA media containing 0.15% of N,N-Dimethyl-p-toluidine (Sigma-Aldrich) was added for polymerization. Polymerization was complete after 12 h. Plastic blocks were stored in a vacuum bag at -20°C until imaging.

Protein localization by fEM [39]: Serial sections (80 nm) were collected onto pre-cleaned coverslips. For fluorescence nanoscopy, photo-activated localization microscopy (PALM; Zeiss, PAL-M, Prototype Serial No. 2701000005) was employed. The region of interest was screened using wide-field illumination. Just prior to PALM imaging, 250 nm gold nanoparicles (Micospheres-Nanospheres), which serve as fiduciary markers, were applied to the sections for 4 min. Then, 3500-5000 frames with an exposure time of 50 ms/frame were collected while stochastically photo-converting mEos signals with 1 μW of a 405 nm laser. For EM imaging,

sections were then stained with 2.5% uranyl acetate (EMS) in water, and a thin layer of carbon was applied. Back-scattered electrons were collected using a scanning electron microscope (FEI, nova nano) and a high contrast solid-state detector (FEI, vCD). Fluorescence and electron micrographs were aligned based on the gold fiduciary markers.

1. Brenner S (1974) The genetics of Caenorhabditis elegans. Genetics 77: 71-94.
2. Riddle DL, Swanson MM, Albert PS (1981) Interacting genes in nematode dauer larva formation. Nature 290: 668-671.
3. Starich TA, Herman RK, Kari CK, Yeh WH, Schackwitz WS et al. (1995) Mutations affecting the chemosensory neurons of Caenorhabditis elegans. Genetics 139: 171-188.
4. Kaletta T, Schnabel H, Schnabel R (1997) Binary specification of the embryonic lineage in Caenorhabditis elegans. Nature 390: 294-298.
5. Michaux G, Gansmuller A, Hindelang C, Labouesse M (2000) CHE-14, a protein with a sterol-sensing domain, is required for apical sorting in C. elegans ectodermal epithelial cells. Curr Biol 10: 1098-1107.
6. Withee J, Galligan B, Hawkins N, Garriga G (2004) Caenorhabditis elegans WASP and Ena/VASP Proteins Play Compensatory Roles in Morphogenesis and Neuronal Cell Migration. Genetics 167: 1165.
7. Nakamura K, Kim S, Ishidate T, Bei Y, Pang K et al. (2005) Wnt signaling drives WRM-1/beta-catenin asymmetries in early C. elegans embryos. Genes Dev 19: 1749-1754.
8. Perkins LA, Hedgecock EM, Thomson JN, Culotti JG (1986) Mutant sensory cilia in the nematode Caenorhabditis elegans. Dev Biol 117: 456-487.
9. Lin K, Hsin H, Libina N, Kenyon C (2001) Regulation of the Caenorhabditis elegans longevity protein DAF-16 by insulin/IGF-1 and germline signaling. Nat Genet 28: 139-145.
10. Harris J, Honigberg L, Robinson N, Kenyon C (1996) Neuronal cell migration in C. elegans: regulation of Hox gene expression and cell position. Development 122: 3117-3131.

11. Eisenmann DM, Kim SK (2000) Protruding vulva mutants identify novel loci and Wnt signaling factors that function during Caenorhabditis elegans vulva development. Genetics 156: 1097-1116.

12. Herman MA, Horvitz HR (1994) The Caenorhabditis elegans gene lin-44 controls the polarity of asymmetric cell divisions. Development 120: 1035-1047.

13. Trent C, Tsuing N, Horvitz HR (1983) Egg-laying defective mutants of the nematode Caenorhabditis elegans. Genetics 104: 619-647.

14. Zinovyeva AY, Forrester WC (2005) The C. elegans Frizzled CFZ-2 is required for cell migration and interacts with multiple Wnt signaling pathways. Dev Biol 285: 447-461.

15. Thorpe CJ, Schlesinger A, Carter JC, Bowerman B (1997) Wnt signaling polarizes an early C. elegans blastomere to distinguish endoderm from mesoderm. Cell 90: 695-705.

16. Ferguson EL, Horvitz HR (1985) Identification and characterization of 22 genes that affect the vulval cell lineages of the nematode Caenorhabditis elegans. Genetics 110: 17-72.

17. Sawa H, Lobel L, Horvitz HR (1996) The Caenorhabditis elegans gene lin-17, which is required for certain asymmetric cell divisions, encodes a putative seven-transmembrane protein similar to the Drosophila Frizzled protein. Genes Dev 10: 2189-2197.

18. Desai C, Garriga G, McIntire SL, Horvitz HR (1988) A genetic pathway for the development of the Caenorhabditis elegans HSN motor neurons. Nature 336: 638-646.

19. Rocheleau CE, Downs WD, Lin R, Wittmann C, Bei Y et al. (1997) Wnt signaling and an APC-related gene specify endoderm in early C. elegans embryos. Cell 90: 707-716.

20. Walston T, Guo C, Proenca R, Wu M, Herman M et al. (2006) mig-5/Dsh controls cell fate determination and cell migration in C. elegans. Dev Biol 298: 485-497.

21. Siegfried KR, Kimble J (2002) POP-1 controls axis formation during early gonadogenesis in C. elegans. Development 129: 443-453.

22. Koga M, Take-uchi M, Tameishi T, Ohshima Y (1999) Control of DAF-7 TGF-β expression and neuronal process development by a receptor tyrosine kinase KIN-8 in Caenorhabditis elegans. Development 126: 5387-5398.

23. Green JL, Inoue T, Sternberg PW (2008) Opposing Wnt pathways orient cell polarity during organogenesis. Cell 134: 646-656.

24. Prasad BC, Ye B, Zackhary R, Schrader K, Seydoux G et al. (1998) unc-3, a gene required for axonal guidance in Caenorhabditis elegans, encodes a member of the O/E family of transcription factors. Development 125: 1561-1568.

25. Pujol N, Bonnerot C, Ewbank JJ, Kohara Y, Thierry-Mieg D (2001) The Caenorhabditis elegans unc-32 gene encodes alternative forms of a vacuolar ATPase a subunit. J Biol Chem 276: 11913-11921.

26. Landmann F, Quintin S, Labouesse M (2004) Multiple regulatory elements with spatially and temporally distinct activities control the expression of the epithelial differentiation gene lin-26 in C. elegans. Dev Biol 265: 478-490.

27. Okkema PG, Harrison SW, Plunger V, Aryana A, Fire A (1993) Sequence requirements for myosin gene expression and regulation in Caenorhabditis elegans. Genetics 135: 385-404.

28. Heiman MG, Shaham S (2009) DEX-1 and DYF-7 establish sensory dendrite length by anchoring dendritic tips during cell migration. Cell 137: 344-355.

29. Perens EA, Shaham S (2005) C. elegans daf-6 encodes a patched-related protein required for lumen formation. Dev Cell 8: 893-906.

30. Wang Y, Apicella A, Lee SK, Ezcurra M, Slone RD et al. (2008) A glial DEG/ENaC channel functions with neuronal channel DEG-1 to mediate specific sensory functions in C. elegans. EMBO J 27: 2388-2399.

31. Bacaj T, Tevlin M, Lu Y, Shaham S (2008) Glia are essential for sensory organ function in C. elegans. Science 322: 744-747.

32. Han K, Levine MS, Manley JL (1989) Synergistic activation and repression of transcription by Drosophila homeobox proteins. Cell 56: 573-583.

33. Mckinney SA, Murphy CS, Hazelwood KL, Davidson MW, Looger LL (2009) A bright and photostable photoconvertible fluorescent protein. Nat Methods 6: 131.

34. Mello CC, Kramer JM, Stinchcomb D, Ambros V (1991) Efficient gene transfer in C. elegans: extrachromosomal maintenance and integration of transforming sequences. EMBO J 10: 3959-3970.

35. Yoshimura S, Murray JI, Lu Y, Waterston RH, Shaham S (2008) mls-2 and vab-3 control glia development, hlh-17/Olig expression and glia-dependent neurite extension in C. elegans. Development 135: 2263-2275.

36. Yu S, Avery L, Baude E, Garbers DL (1997) Guanylyl cyclase expression in specific sensory neurons: a new family of chemosensory receptors. Proc Natl Acad Sci USA 94: 3384-3387.

37. Wicks SR, Yeh RT, Gish WR, Waterston RH, Plasterk RH (2001) Rapid gene mapping in Caenorhabditis elegans using a high density polymorphism map. Nat Genet 28: 160-164.

38. McDonald K (2007) Cryopreparation methods for electron microscopy of selected model systems. Methods Cell Biol 79: 23-56.

39. Watanabe S, Punge A, Hollopeter G, Willig KI, Hobson RJ et al. (2011) Protein localization in electron micrographs using fluorescence nanoscopy. Nat Methods 8: 80-84.